

OblivCDN: A Practical Privacy-preserving CDN with Oblivious Content Access

Viet Vo
Swinburne University of Technology
Melbourne, Australia
vvo@swin.edu.au

Shangqi Lai
CSIRO's Data61
Melbourne, Australia
shangqi.lai@data61.csiro.au

Xingliang Yuan
The University of Melbourne
Melbourne, Australia
xingliang.yuan@unimelb.edu.au

Surya Nepal
CSIRO's Data61
Sydney, Australia
surya.nepal@data61.csiro.au

Qi Li
Tsinghua University
Beijing, China
qli01@tsinghua.edu.cn

ABSTRACT

Content providers increasingly utilise Content Delivery Networks (CDNs) to enhance users' content download experience. However, this deployment scenario raises significant security concerns regarding content confidentiality and user privacy due to the involvement of third-party providers. Prior proposals using private information retrieval (PIR) and oblivious RAM (ORAM) have proven impractical due to high computation and communication costs, as well as integration challenges within distributed CDN architectures.

In response, we present OblivCDN, a practical privacy-preserving system meticulously designed for seamless integration with the existing real-world Internet-CDN infrastructure. Our design strategically adapts Range ORAM primitives to optimise memory and disk seeks when accessing contiguous blocks of CDN content, both at the origin and edge servers, while preserving both content confidentiality and user access pattern hiding features. Also, we carefully customise several oblivious building blocks that integrate the distributed trust model into the ORAM client, thereby eliminating the computational bottleneck in the origin server and reducing communication costs between the origin server and edge servers. Moreover, the newly-designed ORAM client also eliminates the need for trusted hardware on edge servers, and thus significantly ameliorates the compatibility towards networks with massive legacy devices. In real-world streaming evaluations, OblivCDN demonstrates remarkable performance, downloading a 256 MB video in just 5.6 seconds. This achievement represents a speedup of 90× compared to a strawman approach (direct ORAM adoption) and a 366× improvement over the prior art, OblivP2P.

CCS CONCEPTS

• Security and privacy → Privacy-preserving protocols.

Permission to make digital or hard copies of part or all of this work for personal or classroom use is granted without fee provided that copies are not made or distributed for profit or commercial advantage and that copies bear this notice and the full citation on the first page. Copyrights for third-party components of this work must be honored. For all other uses, contact the owner/author(s).
ASIA CCS '25, August 25–29, 2025, Hanoi, Vietnam
© 2025 Copyright held by the owner/author(s).
ACM ISBN 979-8-4007-1410-8/25/08.
<https://doi.org/10.1145/3708821.3710826>

KEYWORDS

Content Delivery Network, Trusted Execution Environment, Oblivious RAM, Distributed Point Function

ACM Reference Format:

Viet Vo, Shangqi Lai, Xingliang Yuan, Surya Nepal, and Qi Li. 2025. OblivCDN: A Practical Privacy-preserving CDN with Oblivious Content Access. In *ACM Asia Conference on Computer and Communications Security (ASIA CCS '25)*, August 25–29, 2025, Hanoi, Vietnam. ACM, New York, NY, USA, 22 pages. <https://doi.org/10.1145/3708821.3710826>

1 INTRODUCTION

Content Delivery Networks (CDNs), such as Netflix [72], Akamai [3], and Cloudflare [27], offer a popular way for file sharing and video streaming. The typical usage of CDNs offloads global traffic from an origin server to edge servers, located close to end-users, and improves the end-user's fetch latency. Such wide adaptation of CDNs is predicted to generate a massive market growth of US\$3.2B by 2026 [78] and serves a large portion (73%) of global traffic [51].

Despite these benefits, CDNs remain significant security concerns regarding content confidentiality and user privacy. Unauthorised data access to CDN contents has been reported frequently [20, 26, 53, 85]. Thus, data needs to be always encrypted to protect content confidentiality in the origin and edge servers. In addition, end-users' privacy can be compromised by exploiting the content access patterns in CDNs [17, 39, 92], even though the content remains encrypted. For example, when end-users repeatedly access the same content from the same server, the content popularity and users' personal interests can be inferred from these access patterns via fingerprinting [17, 39]. The access patterns are also widely exploited in encrypted storage by leakage attacks [18, 52] to infer users' content requests. Therefore, hiding the access patterns of contents is crucial to protect end-users' privacy.

While many privacy-preserving content distribution systems have been proposed [29, 30, 47, 54–56], they often lack compatibility with real-world Internet CDN architecture [3, 27, 72] and struggle to achieve both security and efficiency. For example, APAC [54] considers the peer-assisted CDN setting, which allows a peer node to download the content from edge servers and share content with nearby nodes. However, this work aims to fortify the users' privacy between peers, but still maintain a deterministic access pattern on edge servers. On the other hand, some systems [30, 56] require a

trusted execution environment (TEE) on all edge servers. Unfortunately, TEEs may not always be available due to infrastructure differences among regions. It also hardly updates the infrastructure in an effective and financial way, since existing CDN providers, such as Netflix [72], Akamai [3], and Cloudflare [27], have already deployed thousands of edge servers globally [68].

Although some existing proposals [29, 47, 55] attempt to be compatible with real-world CDN systems, we stress that those works rely on heavy building blocks (e.g., Private Information Retrieval) and introduce a noticeable latency for end-users when downloading content from edge servers. For instance, downloading a 512KB block takes 4.1s with OblivP2P [55] and 2s with Multi-CDN [29] from 2^5 servers, which means a 256MB video could take 35 and 17 minutes to be fully downloaded, respectively. Moreover, those designs require CDN providers to create a significant number of replicas (at least twofold to support multi-server PIR [47, 55] and more to accelerate in [29]) for the entire world of CDN content [32, 33, 37, 91]. This adaptation also increases the bandwidth cost for end-users to download the replicated content from multiple edge servers.

In this study, we propose OblivCDN, a new practical privacy-preserving CDN system. OblivCDN not only addresses the above security concerns but also seamlessly integrates with the real-world CDN architecture. Furthermore, it achieves low-latency oblivious content access without incurring additional bandwidth costs for end-users and storage expenses at the edge servers.

Technique Overview. Our observation is that the real-world CDN architecture can be easily adapted to satisfy our security goals with Oblivious RAM (ORAM) [83], i.e., placing the ORAM client at the origin server/end-user sides and distributing the ORAM server storage among edge servers. However, such a naive solution causes significant latency and bandwidth costs when end-users fetch content. Besides, it also incurs a computational bottleneck at the origin server and prohibitive communication overhead between the edge servers and the origin server.

To reduce end-users' fetch cost, OblivCDN considers the locality of content blocks and decomposes the end-users' requests into multiple range queries for contiguous blocks. We adapt range ORAM [21] to optimise the memory and disk storage on the origin and edge servers, which enables efficient range accesses with no access pattern leakage. Furthermore, to eliminate the computation and communication overhead, OblivCDN separates the metadata and physical video blocks between the origin and edge servers. Specifically, OblivCDN follows existing CDN systems [67, 68] to employ a TEE-enabled origin server to manage only the metadata of video blocks (key and addressing information), while the larger content blocks are stored in separated ORAM storage on the edge servers. The origin server only pushes content blocks to the edges during uploads, and they are never routed back to the origin. As a result, the design of OblivCDN reduces the computation and communication overhead associated with using ORAM in CDNs.

On the other hand, we realise that distinguishing end-users' access patterns on the untrusted edge servers is possible, either through network traffic analysis [17, 39, 92] or attacks on encrypted databases [18, 52]. Obfuscating the access patterns becomes challenging without the presence of a trusted ORAM client deployed in edge servers or duplicating the content and bandwidth costs [16, 36, 95, 97]. OblivCDN introduces a new design to address this challenge.

Specifically, OblivCDN distributes the ORAM trust assumption to two non-colluding computing service nodes located close to the edge servers. These two nodes jointly function as an ORAM client and receive instructions from the origin server to manipulate edge storage with customised oblivious building blocks. The significance of this design lies in its capability to support oblivious range access and protect the access patterns of user content requests without increasing end-user bandwidth or replicating the edge storage.

We implement the prototype for OblivCDN and conduct an extensive evaluation. We first benchmark the performance of oblivious building blocks in OblivCDN. The experiment shows that with these building blocks and video metadata/data separation design, OblivCDN successfully reduces the origin server's communication bandwidth to a constant, which is smaller than 8 MB, regardless of the video block size. Next, we compare the real-world streaming performance of OblivCDN with a Strawman approach, which is a direct ORAM adaption. The results demonstrate that OblivCDN improves 87 – 90× end-users' fetching latency for content between 2 – 256 MB. Regarding communication, OblivCDN saves 6.1 – 786×. Compared to OblivP2P in a setting of 2^5 peers [55], OblivCDN improves end-users' fetch latency by 366× and 40× throughput when requesting a 256MB file. In summary, our contributions are that:

- We propose OblivCDN, the first CDN system designed to protect both content confidentiality and user privacy (access patterns to content) while maintaining compatibility with existing mainstream CDNs [3, 27, 72].
- We formally analyse the security and performance of all entities involved in OblivCDN, including the origin server, edge servers, and non-colluding computing service nodes.
- We extensively evaluate OblivCDN with our Strawman design and OblivP2P [55] under the real-world streaming setting.

2 PRIMITIVE BUILDING BLOCKS

Path ORAM and Data Locality. We leverage range ORAM [21], a variant of Path ORAM [83], to enable efficient oblivious range access on CDN content. Without loss of generality, the Path ORAM contains a storage server and a client. The server maintains a full binary tree with N nodes. Each node contains Z blocks with size B . If a node has less than Z valid blocks, the node will be padded with dummy blocks to ensure that each node has a fixed size ($Z \times B$). The client maintains two data structures: a stash S , which keeps all blocks that are yet to be written to the server (can be blocks fetched from the server or new blocks); a position map position, which keeps the mapping between blocks and the leaf node IDs in the binary tree. The Path ORAM protocol consists of three algorithms:

- $(T, \text{position}, S) \leftarrow \text{ORAM.Init}(N, Z, B)$: Given the tree node number N , node size Z and block size B , the server allocates $N \times Z \times B$ space and arranges it as a full binary tree T with $\lceil \log_2 N \rceil$ levels. The client generates a position map position with random path information and a stash S .
- $\text{ORAM.Access}(\text{Op}, \text{bid}, T, \text{position}, S, b)$: With the binary tree T , the position map position and a block ID bid , the client gets the leaf node ID $\text{lf} \leftarrow \text{position}[\text{bid}]$ from position. Then, it fetches all the blocks from the root of T to lf and decrypts them, and inserts all these blocks into the stash S . If $\text{Op} = \text{'read'}$, the client loads

$S[bid]$ into b . If $Op = \text{'write'}$, the client puts b into $S[bid]$. Meanwhile, it assigns a new random leaf node ID to bid in position to ensure that the next access to this block goes to a random path.

- $ORAM.Evict(T, position, S, lf)$: To write the blocks in S back to a path with the given leaf node lf , the client scans all blocks in S and tries to fit the blocks into the nodes between the leaf node lf to the root node. If a node at the current level has enough space, the client encrypts the block and evicts the encrypted block from the stash to that node. Otherwise, the block remains in the stash. Finally, the nodes are written back to the store on the server.

In Path ORAM, each $ORAM.Access$ always incurs path read operations in a tree path specified by the client. The accessed block will then be assigned with a new random tree path, so even the access on the same block will be randomised on the view of the server-side adversary. Moreover, $ORAM.Evict$ is always invoked after each $ORAM.Access$ to write the accessed path, so the server-side adversary cannot distinguish read and write operations.

Under the CDN context, we specifically want to ensure efficient sequential accesses over data blocks as it is crucial to the streaming performance. Hence, we employ a Path ORAM variant, named range ORAM (rORAM) [21]. In rORAM, the client can have a predefined parameter $R \leq N$ to indicate the maximum sequence size that can be fetched in one access. The server storage will be organised to have $\log_2 R + 1$ separate stores, denoted as E_r , where $r \in [0, \log_2 R]$. The rORAM client also keeps $\log_2 R + 1$ copies of data structures (i.e., $position_r$ and S_r) that are corresponding to each E_r .

In rORAM, each E_r stores 2^r blocks in a way that can serve 2^r sequential range queries with minimised disk seeks while preserving the randomness of blocks not in the targeted range. Moreover, the blocks in each layer of all ORAM trees are stored adjacent to each other, which enables batch eviction that only requires fixed seeks independent of the number of blocks to be evicted.

With rORAM, CDN providers can accelerate sequential access on video blocks and thus improve the service quality in streaming. Particularly, let a video block sequence be $[bid, bid + 2^r)$, and the stash of E_r be S_r . The scheme involves the following operations:

- $E_r.ReadRange(bid)$ allows oblivious access $ORAM.Access$ operation for blocks in the range $[bid, bid + 2^r)$, where $2^r \leq R$. The requested 2^r blocks are loaded into the S_r .
- $E_r.BatchEvict(k)$ loads all blocks from the targeted k paths in E_r to S_r . Then, it writes k paths with blocks from S_r to E_r .

With rORAM, it only requires an $O(\log_2 N)$ disk seeks to retrieve 2^r consecutive blocks and $O(\log_2 N)$ seeks to evict k paths to E_r , regardless of r . As a leakage tradeoff, the optimal access reveals the range size supported by E_r . More details are given in Appendix A.

Intel SGX. Intel SGX is an instruction set to enable hardware-assisted confidential computation [28]. It has been widely adopted by popular cloud platforms (e.g., Azure, AWS) [63]. Despite concerns about memory side-channel leakage [14, 15, 62, 94], numerous techniques readily obfuscate the *Enclave's* access pattern to CPU caches in Intel SGX [74, 76, 80]. Additionally, cloud providers often respond promptly to TEE attacks [64].

Distributed Point Functions. Distributed Point Function (DPF) shares a point function $f(x)$, which evaluates to 1 on the input x^* and to 0 on other inputs, to function shares $f_{i \in [1, m]}$ s.t. $\sum_{i=1}^m f_i(x) = f(x)$ for any input x , while none of the f_i information-theoretically

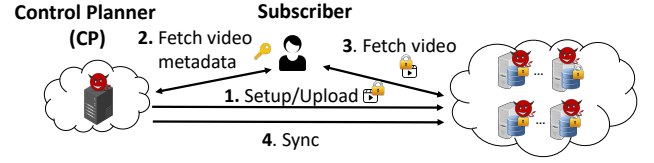


Figure 1: General CDN Architecture

reveals f [12, 13, 42]. Under the two-party setting, the DPF consists of two probabilistic polynomial-time algorithms:

- $Gen(1^\lambda, x^*)$ is a key generation algorithm that takes the security parameter 1^λ and an input x as inputs and outputs a tuple of keys (k_1, k_2) for the point function at x^* .
- $Eval(k_p, x')$ is an evaluation algorithm executed at each party $p \in [1, 2]$, which takes the inputs of k_p and an evaluation point x' , and outputs y_p , where y_p is an additive share of 1 if $x' = x^*$, or a share of 0 otherwise.

Considering the point function as an n -vector with $f(x), x \in [0, n)$, with DPF, the communication cost of sending such a vector is reduced to $O(\log_2 n)$. Moreover, each server only requires $O(n \cdot \log_2 n)$ block cipher operations to obtain the shared vector [13].

3 SYSTEM OVERVIEW

3.1 System Entities and Operations

In this paper, we follow the real-world CDN structure [67, 68] as shown in Figure 1. In specific, a *CDN service provider* (e.g., Netflix) hires a control planner *CP* and a number of edge servers *ESs*. The *CP* is hosted by a *cloud service provider* [67]. The *ESs* are deployed within the network of an *ISP partner* [68]. When a *Subscriber* sends a video request, the *CP* responds by providing the metadata for the requested blocks within the video. Subsequently, the *ESs* transmit sequences of blocks to the *Subscriber*.

Formally, a CDN system contains four operations as follows:

Setup: The *CDN service provider* instructs the *CP* to establish connections to the *ESs* and initialise all required data structures.

Upload: The service provider uploads the video to the *CP*. Then, the *CP* encrypts the video and distributes encrypted blocks to *ESs*.

Fetch: Given a requested video ID, the *CP* responds to the *Subscriber* with the metadata of the video (i.e., decryption keys and the addresses of requested video blocks). Then, the *Subscriber* accesses *ESs* to download the video blocks and finally decrypts them.

Sync: After users' access or video metadata updates from the *CDN service provider*, the *CP* instructs *ESs* to update video blocks.

3.2 Threat Model

Privacy threats. Four parties are involved in the CDN system, i.e., the *CDN service provider*, the *cloud service providers*, the *ISP partners*, and the *Subscriber*. In this paper, we consider the *cloud service providers* and *ISP partners* as untrusted due to frequent data breaches [8, 19, 20, 53, 84, 85, 88]. Specifically, the *cloud service providers* and *ISP partners* are semi-honest, with the condition that they adhere to the Service Level Agreements with the *CDN service provider* [71]. However, they do not collude with each other because

practical CDN deployments often adopt a multi-cloud approach to explore the commercial benefits of various providers [4]¹.

Adversarial Capabilities. Under our assumption, the adversary in the *cloud service providers* and *ISP partners* side can control the *CP* and *ESs*, respectively. In particular, the adversary can access the entire software stack, including the hypervisor and OS of the instance hosting *CP* and *ESs*. They can obtain memory traces from the caches, memory bus, and RAMs, with the sole exception of accessing the processor to extract information. Moreover, the adversary can capture communications with other entities through traffic fingerprinting [17, 39, 92] and by exploiting ISP portals [43, 70].

In addition to software and hardware accesses, the adversary is collecting the access patterns of *Subscribers* on the *CP* and *ESs*. The adversary can leverage the memory access pattern to raise attacks on encrypted storage, such as the leakage abuse attack [18, 52]. On the other hand, the access pattern can be exploited to conduct side-channel attacks against servers with TEE features [14, 44, 45, 96]. We consider that adversaries in the *CP* and *ESs* can arbitrarily create *Subscriber* accounts to collect the aforementioned information.

Defence Assumption. With real-world *CDN service providers* having moved the *CP* to the cloud (e.g., Netflix has moved to AWS [67]), we assume the TEE-enabled cloud instances [5] are generally available. We assume that the CDN deploys the advanced key management mechanism [48] to frequently refresh the video decryption key at a low cost. Furthermore, we note that Byzantine faulty behaviour can be prevented by existing countermeasures [48]. Besides, we assume that the communications between all parties involved in CDN are transmitted via a secure channel.

Defence Limitation. Our design does not address side-channel attacks that exploit speculative execution [89], or implementation bugs [61] against TEE. We consider these attacks to be out of this work, and there are existing solutions available to address them. For instance, MI6 [11] and KeyStone [60] can be employed to handle such attacks. Additionally, hardware providers have the option to release microcode patches to rectify these vulnerabilities [11, 28].

We also do not consider side-channel attacks that exploit traffic bursts such as streaming bit-rate variation [81], or ORAM volume attacks [9]. These specific attacks can be mitigated by complementary works [75] and [57], respectively. Furthermore, our design does not consider attacks involving delay/denying content delivery, misrouting, and distributed DoS attacks [41, 46]. Mainstream CDNs actively investigate and address them on a daily basis [25]. We also do not consider user anonymity (e.g., using Tor) due to copyright obligations from mainstream CDNs [73].

3.3 Formulating Design Goals

For ease of analysis, we will break down practical security goals (SGs), efficiency goals (EGs), and deployment requirements (DR) that align with mainstream CDNs [68] as follows:

SG1: Video Confidentiality. Video blocks of the requested video remain encrypted at the *ESs*. Only the *Subscriber*, who obtains the decryption keys for those blocks from the *CP*, can decrypt them. The keys are refreshed per video request.

SG2: Video Access Patterns. The *ISP partner* cannot know which blocks of which video are sent to the uncompromised *Subscriber*.

¹The collusion is still possible between *ESs* within the same ISP network.

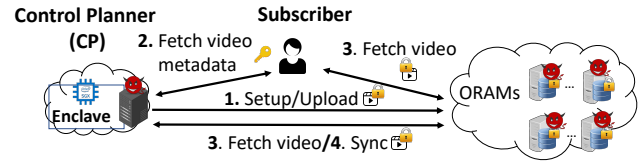


Figure 2: Strawman Design

SG3: Metadata Access Protection. The *cloud service provider* cannot know which video is requested by uncompromised *Subscriber*.

EG1: Efficient Computation. The *CP* does not operate on actual video blocks once the video has been pushed to the *ESs* [27].

EG2: Low Bandwidth Overhead. Video blocks should not be redirected to the *CP* for any purpose, e.g., cryptographic operations, following the current CDN design [68]. Only low bandwidth is required to manipulate video blocks between *ESs* and *CSs*.

EG3: Low Fetch/Sync Latency. The *Subscriber* directly retrieves video blocks in sequential accesses from the *ESs*, and the *ESs* access/update blocks with optimal disk seeks.

DR: CDN Compatibility. With mainstream CDNs moving the *CP* to the clouds [5, 67], we consider the usage of confidential computing (i.e., TEE) in the *CP* to be compatible. However, Internet-CDN infrastructures [3, 27, 72] deployed thousands of *ESs* (e.g., Netflix-OCA devices [72]) globally. To be compatible with legacy devices, we consider the worst case when all *ESs* do not have TEE. Furthermore, we aim to avoid any solutions that rely on massive replicas and huge bandwidth costs when accessing the content to enable our design to be incrementally deployed on existing CDNs.

3.4 A Strawman CDN design using ORAM

With the above assumptions, it is intuitive to have a Strawman design that relies on TEE and Path ORAM solutions [21, 83]. As shown in Figure 2, the Strawman design leverages the *Enclave* within the *CP* as the ORAM client and the ORAM storage is distributed among the *ESs*. The *Enclave* maintains two data structures, namely,

- VideoMap, which stores the map between a video ID vid and the corresponding block identifier list $\{bid_i\}$, $i \in [0, V)$, where V is the number of blocks for a video.
- BlockStateMap, which stores the map between a block identifier bid and its block state (c, l) , where c the latest **counter** for AES encryption/decryption and l is the **path** information from the standard ORAM position map (e.g., $position[bid]$, see Section 2).

, and it instantiates the four CDN operations as follows:

Setup: The *CDN service provider* runs remote attestation with the *CP* to attest the *Enclave* code. Then, the *Enclave* establishes connections to all *ESs* and initialises ORAM trees on *ESs*.

Upload: The *CDN service provider* uploads the video to the *Enclave* through the secure channel established during attestation. The *Enclave* firstly trunks the video into V blocks b_i and assigns those blocks' block states (c_i, l_i) into $BlockStateMap[bid_i]$. Then, the *Enclave* runs $ORAM.Access('write', bid_i, T, l_i, S, b_i)$ to write those video blocks. After running $ORAM.Access$, the video blocks will be placed into the ORAM stash S inside the *Enclave*. The $\{bid_i\}$ list of those blocks will be added into the $VideoMap[vid]$.

Fetch: Given a requested vid , the *Enclave* queries the $VideoMap$ and $BlockStateMap$ and responds to the *Subscriber* the identifier

Table 1: Schemes against design goals in §3.3

	●—fully achieve, ◐—partially achieve, ○—not meet						
Scheme	SG1	SG2	SG3	EG1	EG2	EG3	DR
Strawman	●	●	●	○	○	○	○
rORAM-Strawman	●	●	●	○	○	●	○
Video Data/Metadata Separation	●	◐	●	●	●	●	●
CP with Distributed Trust	●	●	●	●	●	●	●

list $\{bid_i\}$ and the states (c_i, l_i) of the requested video. Then, the *Subscriber* runs $ORAM.Access('read', bid_i, T, l_i, S, b_i)$ for $i \in [0, V)$ to download all video blocks from the *ESs* following the metadata. The *Enclave* also runs the same $ORAM.Access$ operation to download the retrieved blocks into the ORAM stash S on the background and updates the path and counter (c, l) of accessed bid following the Path ORAM protocol accordingly.

Sync: After each $ORAM.Access$ operation, the *Enclave* refers to $BlockStateMap$ to run $ORAM.Evict(T, BlockStateMap, S, l_i)$ and flush the content inside the ORAM stash S into accessed path l_i in the ORAM storage T on *ESs*.

This design can meet all desired security goals (§3.3) as follows:

SG1: All video blocks remain encrypted at the *ESs*. Only the *Enclave* in the *CP* can generate and share decryption keys with *Subscribers*. The video block will be re-encrypted in each **Sync** operation.

SG2: With ORAM, fetched blocks are always re-encrypted and stored in new random ORAM paths. Hence, the *ESs* cannot distinguish which video and its blocks have been accessed (see §2).

SG3: The video metadata is placed inside the *Enclave*, which is inaccessible to the untrusted part of the *CP*. Moreover, we follow prior works ([59, 65, 80], just list a few) to use oblivious data structures (Path ORAM) and operations (see Appendix B.1) to store all data structures (i.e., $VideoMap$, $BlockStateMap$, and ORAM Stash S) inside the *Enclave*. This effectively hides the *Enclave*'s memory access patterns and prevents relevant side-channel attacks [14, 15, 62, 94].

However, we notice that few requirements are partially or hardly achieved under the Strawman design, which include:

EG1: Computation Bottleneck. The *CP* directly manipulates the video block inside the *Enclave*, which causes a non-trivial computation cost in the **Sync** operation.

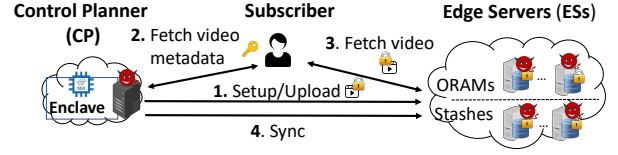
EG2: Intercontinental Bandwidth Blowup. Huge intercontinental communication costs are incurred in **Fetch** and **Sync** operations as the *CP* needs to refresh all accessed blocks within the *Enclave*.

EG3: Long Fetch/Sync Latency. The ORAM incurs an $O(\log_2 N)$ cost [83] to access or evict one block, resulting in a noticeable delay when fetching or synchronising an actual video (with many blocks).

DR: Subscriber Bandwidth Blowup. The Strawman is compatible with the current CDN structure [67, 68], having the TEE on *CP* only. However, *Subscribers* have to download $O(\log_2 N)$ blocks for each targeted video block which leads to a surging bandwidth cost.

4 OBLIVCDN DESIGN

In this section, we present OblivCDN, a CDN system that achieves all design goals set in Section 3.3. We will show our three attempts to gradually refine our design to meet the final requirement. In each attempt, we will elaborate on how we design customised components and integrate them into the CDN system to resolve specific challenges while maintaining other properties. In Table 1, we summarise the security and efficiency of all our designs.

**Figure 3: Video Data/Metadata Separation**

4.1 Attempt 1: rORAM-Strawman

Without changing the system architecture in Figure 2, we can simply achieve the **EG3** requirement by replacing generic the Path ORAM instance with rORAM. In particular, with rORAM, the data structures inside the *Enclave* are modified as follows:

- $VideoMap$ stores the map between a video ID vid and the corresponding block identifier list with ranges $\{(bid_i, r_i)\}, i \in [0, R_V)$, where R_V is the number of ranges generated from the video.

Also, rORAM operations (blue operations) will be invoked instead of generic Path ORAM operations in CDN operations:

Setup: The *CDN service provider* runs remote attestation with the *CP* to attest the *Enclave* code. Then, the *Enclave* establishes connections to all *ESs* and initialises rORAM storage E_r on *ESs*.

Upload: The *CDN service provider* uploads the video to the *Enclave* through the secure channel established during attestation. The *Enclave* firstly trunks the video into V blocks and groups those blocks into R_V ranges with 2^{r_i} consecutive $bids$ starting with bid_i . Their block states $\{(c_i, l_i), \dots, (c_{i+2^{r_i}-1}, l_{i+2^{r_i}-1})\}$ are added into the corresponding entries in $BlockStateMap$. Then, the *Enclave* runs $E_r.ReadRange(bid_i)$ to write those video blocks. After running $E_r.ReadRange$, the video blocks will be placed into the rORAM stash S_r inside the *Enclave*. The $\{(bid_i, r_i)\}$ list of those blocks will be added into the $VideoMap[vid]$.

Fetch: Given a requested vid , the *Enclave* queries the $VideoMap$ and $BlockStateMap$ and responds to the *Subscriber* the identifier list $\{(bid_i, r_i)\}$ and the states $\{(c_i, l_i), \dots, (c_{i+2^{r_i}-1}, l_{i+2^{r_i}-1})\}$ of the requested video. Then, the *Subscriber* runs $E_r.ReadRange(bid_i)$ for $i \in [0, R_V)$ to download all video blocks from the *ESs* following the metadata. The *Enclave* also runs the same $E_r.ReadRange$ operation to download the retrieved blocks into the rORAM stash S_r on the background and update the path and counter (c, l) of accessed $bids$ following the rORAM protocol accordingly.

Sync: After each $E_r.ReadRange$ operation, the *Enclave* refers to $BlockStateMap$ to run $E_r.BatchEvict(2^r)$ and flush the content inside the rORAM stash S_r into 2^r accessed paths into the rORAM storage E_r on *ESs*.

As a result, **EG3** can be fully satisfied as follows:

EG3: With rORAM, the *Subscriber* can fetch required video blocks in sequence after only $O(\log_2 N)$ seeks on targeted *ESs*, independent of the number of blocks requested. The *CP* can also update the video block in batch with optimal $O(\log_2 N)$ disk seeks.

4.2 Attempt 2: Video Data/Metadata Separation

Overview. In the Strawman and rORAM-Strawman approaches, one major bottleneck is the substantial computational and communication costs associated with synchronising video blocks between *CP* and *ESs*. Also, *Subscribers* incur a huge bandwidth cost ($O(2^r \times \log_2 N)$) to fetch targeted 2^r video blocks. In order to achieve

Table 2: Data structures in CDN Entities after Separating Video Data and Metadata

Control Plane (CP)	Enclave	MetaStash _r and BlockTracker _r , $r \in [0, \log_2 R]$ VideoMap and BlockStateMap
Edge Servers (ESs)	E_r S_r	ORAM supports 2^r sequential blocks access The corresponding stash of E_r

EG1, **EG2** and **DR**, we devise a customised rORAM protocol and integrate it into the CDN system to minimise the computation and communication between *CP* and *ESs*, as well as the bandwidth cost for *Subscribers* to download video blocks.

As shown in Figure 3, there are two major changes upon the rORAM-Strawman design: First, we split the *ESs* into two groups with an equal amount of instances. While the first group of those instances still host rORAM storage E_r as in the rORAM-Strawman, the second instance group is dedicated to hosting the rORAM stash S_r of each rORAM storage. This design allows the *CP/Subscribers* to outsource all real video data and operations to *ESs* and thus avoids expensive data block manipulation inside the *Enclave* and bandwidth cost between *CP* and *ESs* as well as *Subscribers* and *ESs*.

To foster the first change, we introduce several new data structures on the *CP* to manage the metadata of CDN videos. Those data structures keep track of the real video blocks' location information and assist the *CP* in instructing *ESs* to manipulate real video blocks without retrieving them. With the new data structure, when the *CP* receives any **Fetch** requests from the *Subscriber*, it lets the *Subscriber* obtain real video blocks from *ESs* via rORAM operations while performing the same **Fetch** operation on the metadata. Later, when the *CP* executes the **Sync** operation, the *Enclave* performs ORAM eviction on the metadata and then remotely *instructs* the *ESs* to keep the ORAMs storing actual video blocks synchronised.

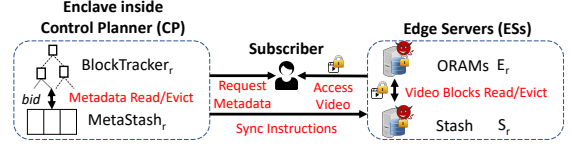
New Data Structures. To implement the above design, we introduce crucial data structures as outlined in Table 2. We now detail the design rationale of these structures as follows:

On the *ES* side, each *ES* will be assigned to host the rORAM storage E_r or the stash S_r on the *ESs*, where $r \in [0, \log_2 R]$. The *ESs* for the rORAM storage still initialises E_r , where $r \in [0, \log_2 R]$, to enable access to 2^r sequential video blocks following the rORAM scheme (§2). On the other hand, the *ESs* for the rORAM stash have the predefined parameters for stash size and its counterpart *ESs* with E_r , so it can generate S_r and pair with a specific E_r to execute E_r .ReadRange and E_r .BatchEvict on behalf of the *CP/Subscribers*².

On the *CP* side, we utilise a small memory within the *Enclave* to store the metadata for E_r and S_r , denoted as BlockTracker_r and MetaStash_r, respectively. As shown in Figure 4, each BlockTracker_r and MetaStash_r have the same ORAM and stash sizes and structure as their counterpart E_r and S_r on *ESs*. The only difference is that BlockTracker_r and MetaStash_r store the video block identifiers (*bid*), while E_r and S_r store the actual video blocks. These meta structures facilitate the following oblivious accesses:

- **MetaData_r.ReadRange(*bid*)**: Load a list of 2^r block identifiers [*bid*, *bid* + 2^r) from BlockTracker_r to MetaStash_r following rORAM ReadRange.

²With S_r on *ESs*, the stash only stores the encrypted video blocks fetched from E_r to preserve **SG1**. The *Subscribers* will keep the decryption counters *c* locally after receiving block states from *CP* and use them decrypt the video blocks from S_r .

**Figure 4: New Data Structures and Updated Operations with Separated Video Data/Metadata**

- **MetaData_r.BatchEvict(*k*)**: Write *k* paths in BlockTracker_r with block identifiers from MetaStash_r following rORAM BatchEvict.

The use of these meta structures enables the *Enclave* to perform the range ORAM access/eviction locally within the *CP* without manipulating CDN video blocks stored in the *ESs*. Specifically, the *Enclave* monitors the routing traces of blocks between the BlockTracker_r and stash_r with **Upload** and **Fetch** operations. After that, these traces enable the *Enclave* to execute logical eviction over *bids* in MetaStash_r and run the **Sync** operation with the *ESs* to perform the same eviction on video blocks with much shorter instructions.

Updated CDN Operations. As shown in Figure 4, the CDN operations will be updated with new data structures. Particularly, **blue** operations are used compared to the rORAM-Strawman as follows: **Setup**: The *CDN service provider* runs remote attestation with the *CP* to attest the *Enclave* code. Then, the *Enclave* establishes connections to all *ESs* and initialises E_r and S_r on *ESs*.

Upload: The *CDN service provider* uploads the video to the *Enclave* through the secure channel established during attestation. The *Enclave* firstly trunks the video into *V* blocks and groups those blocks into R_V ranges with 2^{r_i} consecutive *bids* starting with bid_i . The *Enclave* runs the **MetaData_{r_i}.ReadRange(*bid*_{*i*})** to put *bids* in the range starting with bid_i into MetaStash_{*r_i*}. Their block states $\{(c_i, l_i), \dots, (c_{i+2^{r_i}-1}, l_{i+2^{r_i}-1})\}$ are added into the corresponding entries in BlockStateMap. Then, the *Enclave* runs E_{r_i} .ReadRange(bid_i) to write those video blocks. After running E_{r_i} .ReadRange, the video blocks will be **encrypted and placed into the S_r inside the *ESs***. The $\{(bid_i, r_i)\}$ list of those blocks will be added into the VideoMap[*vid*]. **Fetch**: Given a requested *vid*, the *Enclave* queries the VideoMap and BlockStateMap and responds to the *Subscriber* the identifier list $\{(bid_i, r_i)\}$ and the states $\{(c_i, l_i), \dots, (c_{i+2^{r_i}-1}, l_{i+2^{r_i}-1})\}$ of the requested video. Then, the *Subscriber* runs E_{r_i} .ReadRange(bid_i) for $i \in [0, R_V)$ to instruct *ESs* to **load video blocks from E_r to S_r** . The *Subscriber* can directly download the video blocks from *ESs* with S_r . Meanwhile, the *Enclave* runs **MetaData_{r_i}.ReadRange(*bid*_{*i*})** to load *bids* of the retrieved blocks into the MetaStash_{*r_i*} on the background and update the path and counter (*c*, *l*) of accessed *bids* following the rORAM protocol accordingly.

Sync: After each **ReadRange** operation, the *Enclave* follows the BlockStateMap to run the **MetaData_r.BatchEvict(2^r)** protocol to simulate the eviction on accessed *bids*. Then, the *Enclave* follows the eviction result in the BlockTracker_r to send instructions (i.e., refreshed AES-CTR masks and disk locations generated from the block state (*c*, *l*)) to *ESs* with S_r . Those *ESs* will re-encrypt video blocks and place them in designated locations inside E_r on *ESs*.

This attempt is promising to minimise the intercontinental communication cost, as *CP* only sends short instructions to *ESs*. It also allows *Subscribers* to only download 2^r required video blocks from

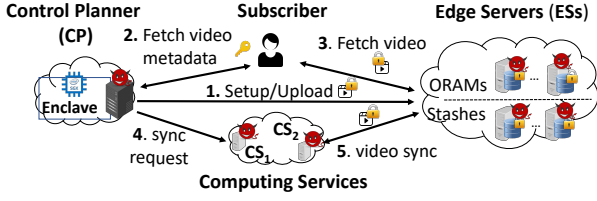


Figure 5: CP with Distributed Trust

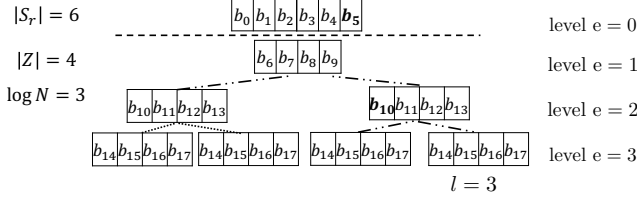


Figure 6: OblivCDN labels blocks with the index b_s format, where s signifies the block order. With the stash size $|S_r| = 6$ and a 8-node ORAM tree with node size $Z = 4$, $s \in [0, 17]$ (0 to $|S_r| + \log_2 N \times Z - 1$) will be assigned to blocks in the stash and each path in an ascending order.

ESs because the ORAM access has been done between ESs. However, we realise that the attempt introduces new security threats. This is because the read/write instructions from the CP reveal the original storage location of a block inside the stash and the next location to write it to ESs. Since ESs are deployed by a semi-honest party, i.e., the ISP partner, this is a direct violation of the SG2 requirement. Although this can be remedied by employing TEE with oblivious primitives on ESs, it also causes compatibility issues, since we do not expect ISP partners to equip their legacy devices with TEE (DR).

4.3 Attempt 3: CP with Distributed Trust

Overview. In Attempt 2, the core design is to delegate a part of the rORAM client to ESs to alleviate the communication cost. However, as we discussed above, this design violates the trust assumptions in §3.2. To resolve this issue, our goal is to allow the party who manipulates video blocks to follow CP’s instructions without knowing them, thus removing the trust requirement on that party.

As shown in §3, real-world CDN service providers have actively sought to deploy the CDN service with multiple cloud providers [4]. In light of this observation, we consider integrating the distributed trust model [32, 33, 37] into CDN systems to make a secure split on CP functionality. Particularly, two semi-honest servers, denoted as computing service node CSs (CS_1 and CS_2), are hired from non-colluding cloud service providers or ISP partners³ that are close to Subscribers (see Figure 5). The CDN service provider delegates CP’s ORAM read/write operations into CSs by instructing them to run oblivious video block routing protocols devised for CDN systems. The new design preserves the benefits of separating video data/metadata. Moreover, it ensures that, as far as the adversary can only compromise one CS, he/she cannot learn the video access pattern. This security guarantee is valid even if the adversary is on the ISP partner side, i.e., can compromise one CS and ESs.

³The non-colluding assumption can be effectively achieved with local law and conflict of interests, especially for two providers in the same region [58].

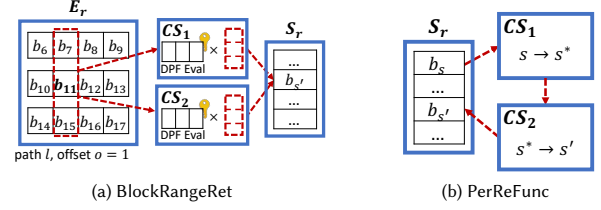


Figure 7: Examples on how to manipulate one block under our rORAM ReadRange design with distributed trust.

Video Block ID Allocation. To enable oblivious video block routing, our insight is that for a tree-based ORAM, it is always has a fixed number of blocks ($|S_r| + \log_2 N \times Z$) in the stash and a given path while the required block is hidden in those blocks. Therefore, if we assign a unified block ID to those blocks, we can locate the required block by a given path and ID. In particular, as shown in Figure 6, we denote each block in ORAM as b_s , where s signifies block order in the path, which is determined as follows:

- (1) The stash occupies the $s \in [0, |S_r|]$.
- (2) For each path, the block will be assigned with s in ascending order from $|S_r|$ to $|S_r| + \log_2 N \times Z - 1$.

We can easily target a specific block with its path and the newly-added ID, i.e., if $s < |S_r|$, we can find it in the s position at the stash. Otherwise, we can use s to compute its level e via $[(s - |S_r|) / Z] + 1$ and offset o in the level by $(s - |S_r|) \% Z$. For instance, b_5 is at the 5th position in the stash, and b_{10} in path $l = 3$ is at the 0 position of the second level at path $l = 3$ according to the setting in Figure 6.

We then adapt the BlockStateMap to store the map between a block identifier bid and the block state (c, l, s) , which enables the CP to compute the block location in path l with the block state.

Oblivious Block Routing. The unified block ID in the path enables the CP to generate instructions for two CSs to jointly function as a rORAM client. In particular, for E_r .ReadRange operations, we consider it as a two-step process, i.e., 1) fetching 2^r blocks from E_r to S_r and 2) accessing S_r for required blocks.

For the block fetching process, each targeted path can be represented as a vector with $\log_2 N \times Z$ elements, while the CP knows the exact location of targeted video blocks in that path. Therefore, we can convert each block fetching process to a PIR process that aims to retrieve one block from a fixed offset at the targeted path in E_r . We implement the following BlockRangeReturn operation with DPF operations (see §2) that enables efficient ReadRange from E_r under the CP with distributed trust setting:

4.3.1 BlockRangeReturn. BlockRangeRet obliviously routes video blocks from E_r to S_r without revealing which specific blocks are being routed to both the E_r to S_r , as well as to each of $CS_{p \in \{1,2\}}$.

We use an example of BlockRangeRet in Figure 7a to demonstrate how it proceeds. In the example, b_{11} ($s = 11$), which is encrypted with counter c under the AES-CTR mode, is routed from E_r to the new address s' in S_r and re-encrypted with c' as follows:

On the Enclave:

- (1) Generates (k_1, k_2) with $\text{DPF.Gen}(1^\lambda, 11)$.
- (2) Computes the re-encryption mask $m = G(c) \oplus G(c')$ with $\text{PRF } G(\cdot)$ and shares it as m_1 and m_2 , where $m_1 \oplus m_2 = m$.
- (3) Computes the offset $o = 1$ with $Z = 4$ and $\log N = 3$.

- (4) Gives the instruction (k_p, m_p, l, o, s') to the query party (can be either the *Enclave* in **Upload** or the *Subscribers* in **Fetch**), who then sends the instruction to $CS_{p \in \{1,2\}}$.

On each $CS_{p \in \{1,2\}}$:

- (1) Executes $y[1] \leftarrow \text{DPF.Eval}(k_p, 7)$, $y[2] \leftarrow \text{DPF.Eval}(k_p, 11)$, $y[3] \leftarrow \text{DPF.Eval}(k_p, 15)$ (i.e., $y[e] \leftarrow \text{DPF.Eval}(k_p, |S_r| + (e - 1) \times Z + o)$, $e \in [1, \log N]$) for all block IDs in the offset.
- (2) Retrieves corresponding encrypted blocks (b_7, b_{11}, b_{15}) from the path l on E_r into vector b .
- (3) Computes shared block b_{11} with $b_p \leftarrow \bigoplus_{e=1}^{\log N} (y[e] \times b[e])$.
- (4) Re-encrypts the share with shared key $b_p \leftarrow b_p \oplus m_p$.
- (5) Jointly writes $b_1 \oplus b_2 = b_{11} \oplus G(c) \oplus G(c')$ into the s' position on S_r , so the original mask $G(c)$ on b_{11} will be canceled and replaced with $G(c')$.

BlockRangeRet efficiently protects the targeted block against adversaries who can compromise one CS and ES s at most since all blocks in the same offset of the path are accessed (no access pattern leakage). Moreover, the final block will be re-encrypted before loading into S_r , so the adversary on ES s cannot correlate the blocks from E_r to that on S_r . We note that BlockRangeRet can execute in a batch setting of 2^r video blocks. This setting optimises disk seeks on E_r and saves communication costs between E_r and $CS_{p \in \{1,2\}}$. Algorithm 4 in Appendix B presents BlockRangeRet in detail.

For the stash access process, we should stress that the major difference between ReadRange in the original rORAM and our design is that the stash is also placed in an untrusted party where the access pattern should also be suppressed. Therefore, we design one extra primitive to Permute and Re-encryption blocks inside S_r after $CP/Subscribers$ accessing S_r for specific blocks.

4.3.2 Permute Re-encryption Function. PerReFunc permutes and re-encrypts all video blocks in S_r following the meta structure MetaStash_r in the *Enclave* of the CP .

Since all blocks in S_r will be permuted and re-encrypted in the same way, we leverage an example from Figure 7b to demonstrate the state of S_r before and after the execution for one block. In this example, the block was encrypted with counter c and will be relocated from address s to s' and re-encrypted with the counter c' :

On the Enclave:

- (1) Selects a permutation with intermediate location, $\omega_1 = s \mapsto s^*$ and $\omega_2 = s^* \mapsto s'$.
- (2) Computes the re-encryption mask $m = G(c) \oplus G(c')$ with PRF $G(\cdot)$ and shares it as m_1 and m_2 , where $m_1 \oplus m_2 = m$.
- (3) Send (ω_p, m_p) to $CS_{p \in \{1,2\}}$.

On CS_1 :

- (1) Retrieves encrypted block b_s from S_r .
- (2) Re-encrypts b_s with shared key $b_s \leftarrow b_s \oplus m_1$.
- (3) Uses ω_1 to permute b_s to b_{s^*} and sends to CS_2 .

On CS_2 :

- (1) Re-encrypts b_{s^*} with shared key $b_{s^*} \leftarrow b_{s^*} \oplus m_2$.
- (2) Uses ω_2 to permute b_{s^*} to $b_{s'}$ and sends to S_r .

After the execution, neither ES s nor $CS_{p \in \{1,2\}}$ can distinguish which blocks have been relocated to which locations. This ensures that the access pattern on S_r is hidden after $CP/Subscribers'$ access from S_r . Algorithm 5 in Appendix B presents PerReFunc in detail.

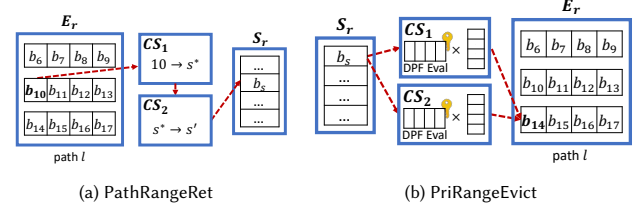


Figure 8: Examples on how to manipulate one block under our rORAM BatchEvict design with distributed trust.

Similarly, we also decompose the E_r .BatchEvict operation into two steps: 1) fetch all blocks from E_r 's targeted paths to S_r ; 2) evict blocks from S_r to E_r following the new block state.

The block fetching process for the eviction is simpler because it inherently requires to access all blocks in each targeted path. Hence, we can consider it as the PerReFunc function between E_r and S_r , which can be implemented with the following protocol:

4.3.3 PathRangeReturn. PathRangeRet privately routes blocks from E_r to S_r without revealing which specific blocks from E_r are being routed to which locations in S_r . During the routing, neither of $CS_{p \in \{1,2\}}$ knows the origin or destination of the blocks.

An example of PathRangeRet is illustrated in Figure 8a. In this example, block b_{10} is re-encrypted and written to s in S_r :

On the Enclave:

- (1) Selects a permutation with intermediate location, $\omega_1 = 10 \mapsto s^*$ and $\omega_2 = s^* \mapsto s$.
- (2) Computes the re-encryption mask $m = G(c) \oplus G(c')$ with PRF $G(\cdot)$ and shares it as m_1 and m_2 , where $m_1 \oplus m_2 = m$.
- (3) Sends (ω_p, m_p) to $CS_{p \in \{1,2\}}$.

On CS_1 :

- (1) Retrieves encrypted block b_{10} from E_r .
- (2) Re-encrypts b_{10} with shared key $b_{10} \leftarrow b_{10} \oplus m_1$.
- (3) Uses ω_1 to permute b_{10} to b_{s^*} and sends to CS_2 .

On CS_2 :

- (1) Re-encrypts b_{s^*} with shared key $b_{s^*} \leftarrow b_{s^*} \oplus m_2$.
- (2) Uses ω_2 to permute b_{s^*} to b_s and sends to S_r .

PathRangeRet can also be executed in a batch setting, processing all blocks in 2^r ORAM paths with the same process. Algorithm 6 in Appendix B presents PathRangeRet in detail.

We then can leverage a reverse process of BlockRangeRet to route the blocks in S_r back to E_r with a similar PIR process with DPF evaluations as in the following protocol:

4.3.4 PrivateRangeEviction. PriRangeEvict routes video blocks from S_r to E_r without revealing which specific blocks are written to which addresses in E_r . During the routing, both the origin and destination of the blocks remain hidden from each of $CS_{p \in \{1,2\}}$.

Figure 8b shows an example of routing the encrypted block b_s to a specific address b_{14} ($s = 14$) in E_r , which proceeds as follows:

On the Enclave:

- (1) Generates (k_1, k_2) with $\text{DPF.Gen}(1^\lambda, s)$.
- (2) Computes the re-encryption mask $m = G(c) \oplus G(c')$ with PRF $G(\cdot)$ and shares it as m_1 and m_2 , where $m_1 \oplus m_2 = m$.
- (3) Sends $(k_p, m_p, l, s = 14)$ to $CS_{p \in \{1,2\}}$.

On each $CS_{p \in \{1,2\}}$:

Algorithm 1 OblivCDN System OperationsSETUP

Input: The addresses of ESs and CSs; The number of nodes N , The number of blocks for each node Z , and The block size B for each rORAM tree; The maximum range R supported by rORAM; The stash size $|S_r|$, $r \in [0, \log_2 R]$ for each stash.

- 1: The *CDN service provider* runs remote attestation with the *CP* to attest the *Enclave* code.
- 2: The *Enclave* initialises all metadata structures. The VideoMap and BlockStateMap are initialised as Path ORAM with $N \times Z \times B$ space. The $\log_2 R + 1$ BlockTracker $_r$ with $N \times Z$ blocks for $bids$ is set for corresponding rORAM tree, and $|S_r|$ space for $bids$ is allocated for $\log_2 R + 1$ MetaStash $_r$.
- 3: The *Enclave* establishes connections to all ESs and initialise $\log_2 R + 1$ rORAM storage E_r with $N \times Z \times B$ space and stash S_r with $|S_r|$ space on ESs.
- 4: The *Enclave* establishes connections to all CSs.

UPLOAD

Input: A video and its *vid*

1. The *CDN service provider* uploads the video to the *Enclave* through the secure channel established during attestation.
2. **On the Enclave:**
 - Trunks the video into V blocks with size B .
 - Groups those blocks into R_V ranges, each range starts with bid_i and contains 2^{r_i} consecutive $bids$ (i.e., $bid_i, bid_i + 1, \dots, bid_i + 2^{r_i} - 1$).
 - For each range, initialises BlockStateMap[bid_a] = (c_a, l_a, s_a) for $a \in [i, i + 2^{r_i})$, where $c_a \leftarrow 0$, $l_i \xleftarrow{\$} [0, \frac{N}{2})$, $l_a \leftarrow (l_{a-1} + 1) \bmod \frac{N}{2}$, and $s_a \xleftarrow{\$} [0, |S_{r_i}|)$, ensuring that if $a \neq a'$, $s_a \neq s_{a'}$.
 - For each range, stores bid_a for $a \in [i, i + 2^{r_i})$ into MetaStash $_{r_i}[s_a]$.
 - For each range, follows BlockStateMap[bid_a] to encrypt the block b_a for $a \in [i, i + 2^{r_i})$ and write into S_{r_i} .
 - Stores the $\{(bid_i, r_i)\}$, $i \in [0, R_V)$ list into VideoMap[*vid*].
 - Invoke the **Sync** operation.

FETCH

Input: A video id *vid*

1. The *Subscriber* sends the video id *vid* to the *Enclave*.
2. **On the Enclave:**
 - Reads VideoMap[*vid*] to obtain $\{(bid_i, r_i)\}$, $i \in [0, R_V)$ and sends to the *Subscriber*.
 - For each range, reads BlockStateMap[bid_a] = (c_a, l_a, s_a) for $a \in [i, i + 2^{r_i})$ and sends to the *Subscriber*.
3. **On the Subscriber's Client:**
 - For each range, refers to BlockStateMap[bid_a] = (c_a, l_a, s_a) for $a \in [i, i + 2^{r_i})$ to compute the location of b_a , i.e., if $s_a < |S_{r_i}|$, then b_a is on the position s_a of S_r ($l_a = 0, e_a = 0, o_a = s_a$); otherwise, b_a is at the level $e_a = \lfloor (s_a - |S_{r_i}|) / Z \rfloor + 1$ of the path l_a of E_r , and its offset o_a in the level is $(s - |S_{r_i}|) \% Z$.
 - For each range, directly downloads b_a with address $(E_{r_i}, S_{r_i}, l_a, e_a, o_a)$ for $a \in [i, i + 2^{r_i})$ and decrypts b_a with c_a .
 - Notifies ESs once download finished.
4. **On the Enclave (Run simultaneously with Step 3):**
 - Refers to $\{(bid_i, r_i)\}$, $i \in [0, R_V)$ to run MetaData $_{r_i}$.ReadRange(bid_i).
 - For each bid loaded into MetaStash $_{r_i}$, refers to BlockStateMap[bid] = (c, l, s) to run BlockRangeRet between E_{r_i} and S_{r_i} , and update (c, l, s) .
 - For each range, permutes the MetaStash $_{r_i}$.
 - Follow the permutation to instructs CSs to run PerReFunc on S_{r_i} and update (c, s) for each bid in MetaStash $_{r_i}$.
 - Invoke the **Sync** operation.
4. **On the ESs:**
 - Replace E_r and S_r with shuffled version after sufficient number of *Subscribers* finishes download or same content is requested.

SYNC

1. **On the Enclave:**

- For each range $r \in [0, \log_2 R]$, check whether 2^r paths have been accessed on BlockTracker $_r$, skip the following steps if the condition is not met.
- Runs MetaData $_r$.BatchEvict(2^r), which firstly loads all $bids$ in 2^r accessed paths into MetaStash $_r$.
- For each bid loaded into MetaStash $_r$, refers to BlockStateMap[bid] = (c, l, s) to run PathRangeRet between E_r and S_r , and update (c, s) .
- Refers to BlockStateMap[bid] = (c, l, s) to continually run MetaData $_r$.BatchEvict(2^r), which writes 2^r accessed path of BlockTracker $_r$ with $bids$ from MetaStash $_r$.
- Follow the eviction process to instructs CSs to run PriRangeEvict to evict blocks from S_r to E_r and update (c, s) for each valid bid evicted from MetaStash $_r$.

- (1) Executes $y[i] \leftarrow \text{DPF.Eval}(k_p, i)$ for all block ID $s \in [0, |S_r|)$ in the stash.
- (2) Retrieves the entire stash from S_r into vector b .
- (3) Computes shared block b_s with $b_p \leftarrow \bigoplus_{i=0}^{|S_r|-1} (y[i] \times b[i])$.
- (4) Re-encrypts the share with shared key $b_p \leftarrow b_p \oplus m_p$.
- (5) Jointly writes $b_1 \oplus b_2 = b_s \oplus G(c) \oplus G(c')$ into the b_{14} position on the path l of E_r , so the original mask $G(c)$ on b_s will be canceled and replaced with $G(c')$.

With E_r .BatchEvict, all blocks in the targeted 2^r paths will be rewritten in batch to ensure the obliviousness of evictions. Algorithm 7 in Appendix B presents PriRangeEvict in detail.

Remarks. In the above design, we consider that the *CP/Subscribers* need to wait for CSs to route blocks from E_r to S_r before accessing those blocks, and thus incurs an extra delay for the process.

Nonetheless, we realise that the CDN service is a typical “read-only” service whose content will never be changed but only shuffled after the initial upload to the cloud. This means we can follow [86] to perform reads directly on the given address and use another background thread to obliviously route the blocks into a new memory space. By the end of each range access, we replace the current rORAM tree E_r with the new one and thus waive the waiting time for each access. Such an approach can be extended to support multi-users by combining distinct video access into one batch.

At the end of this section, we present the full system operations of OblivCDN in Algorithm 1. Note that all vector accesses (i.e., access stashes for VideoMap and BlockStateMap) inside the *Enclave* are done by the oblivious operations in Appendix B.1.

4.4 Theoretical Complexity

Intercontinental Communication Cost. The intercontinental Communication costs in OblivCDN can be divided into 1) the cost of uploading videos, and 2) the cost of sending oblivious block routing instructions to CSs. As in existing CDN systems [67, 68], uploading a video is a one-time cost and linear to the video size. Moreover, the cost of sending instructions can be depicted as:

- In BlockRangeRet, communication with each $CS_{p \in \{1,2\}}$ is dominated by the DPF key size $\log_2(\log_2 N \times Z + |S_r|) \times \lambda$ bits ($O(r)$).
- In PerReFunc, communication with each $CS_{p \in \{1,2\}}$ is bounded by $|S_r| = 2^r \times v$ ($O(2^r)$), where v is the fixed-size stash factor [21].
- In PathRangeRet, communication with each $CS_{p \in \{1,2\}}$ is bounded by the number of blocks in a path, which is $\log_2 N \times Z$ ($O(\log_2 N)$).
- In PriRangeEvict, communication with each $CS_{p \in \{1,2\}}$ is dominated by the DPF key size $\log_2(\log_2 N \times Z + |S_r|) \times \lambda$ bits ($O(r)$).

As a result, the entire intercontinental communication cost (considering each rORAM operation manipulates 2^r paths/blocks in batch) for instructing rORAM operations is $O(r \times 2^r)$ (for ReadRange) and $O(r \times 2^r \times \log_2 N)$ (for BatchEvict) regardless of the block size/video size. In the real-world CDN, the video size is always much larger than the instruction size because a smaller r (e.g., $r = 8$) is already enough for most cases. Hence, compared to loading the video back to the CP in the Strawman design, OblivCDN significantly reduces the intercontinental communication cost without compromising security guarantees. We will demonstrate the benefit of our design with real-world video access scenarios in §5.

Local Region Communication Cost. In the local region, the communication costs can be divided into 1) the cost of fetching videos, and 2) the cost of routing video blocks between ESs and CSs. Since we follow the read-only ORAM design [86] to provide the video service, the communication cost for *Subscribers'* fetches remains unaltered compared to existing CDN systems [67, 68].

Regarding the communications between ESs and CSs, in the **Fetch** operation, $CS_{p \in \{1,2\}}$ firstly acquires $2^r \times \log_2 N \times B$ bytes from ESs and writes $2^r \times B$ bytes back in BlockRangeRet, and then reads/writes $2^r \times v \times B$ bytes in PerReFunc. In the **Sync** operation, $CS_{p \in \{1,2\}}$ firstly reads/writes $2^r \times \log_2 N \times Z \times B$ bytes with ESs in PathRangeRet. Then, it reads $2^r \times v \times B$ bytes from ESs and tries to fill ESs with E_r by $2^r \times \log_2 N \times Z \times B$ bytes via PriRangeEvict.

The above analysis shows that our design maintains a comparable bandwidth cost ($O(2^r \times v)$) against the original rORAM ($O(2^r \times \log_2 N)$) [21] while ensuring the obliviousness of all operations.

Disk Seek on ESs. In both **Fetch** and **Sync** operations, each E_r still takes $O(\log_2 N)$ seeks to fetch 2^r blocks and evict 2^r paths.

Computation Cost. The computation cost in the OblivCDN is minimised, as it only requires evaluating block cipher, permutation, and exclusive-or operations among all components. To be specific, there are 2^r DPF keys and re-encryption masks to be generated and evaluated under BlockRangeRet, and $2^r \times v$ permutations and re-encryption masks for PerReFunc during ReadRange. Also, $2^r \times \log_2 N \times Z$ DPF keys/permutations and re-encryption masks are generated and used for PathRangeRet and PriRangeEvict.

4.5 Security Guarantees

As mentioned in §3.2, OblivCDN follows real-world CDN systems [67, 68] to consider four parties, i.e., the *CDN service provider*,

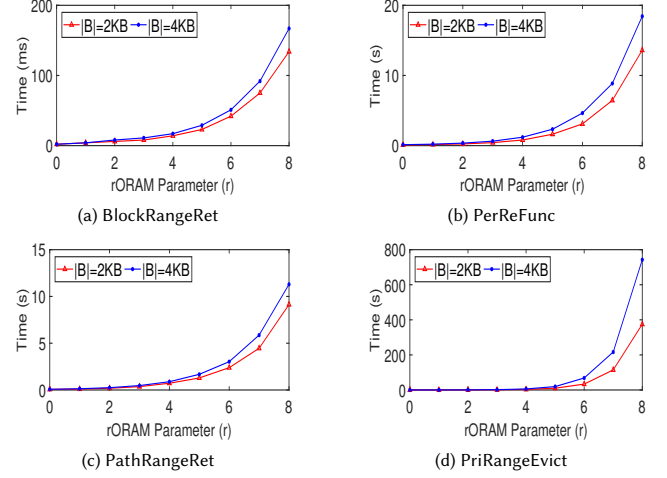


Figure 9: Computational cost of oblivious operations.

the *cloud service providers*, the *ISP partners*, and the *Subscriber*. OblivCDN guarantees that the content and the access pattern of all same-length videos will be indistinguishable against: the *CDN service providers* who host the CP and one CS, and the *ISP partners* who host ESs and potentially also control one CS. Due to the page limitation, we provide a detailed security analysis in Appendix C.

5 EXPERIMENT AND EVALUATION

5.1 Setup

Implementation. We developed the CP and CSs using C++, while the ESs were implemented in Java. The ESs serve as storage daemons for memory/hard drive I/O access as requested. To facilitate communication between these entities, we employed Apache Thrift. For the implementation of the *Enclave* within the CP and DPF scheme, we utilised Intel SGX and Intrinsic, respectively. For cryptographic primitives, such as PRF, PRG, and AES, we used the OpenSSL. Overall, the prototype comprises 48,272 LOC⁴.

Platform. We used three devices to deploy OblivCDN. A server equipped with an Intel Xeon E2288G 3.70GHz CPU (8 cores) and 128GB RAM serves as the ESs. One SGX-enabled workstation featuring an Intel Core i7-8850H 2.60GHz CPU (6 cores) and 32GB RAM functions as the CP. Another workstation with the same configuration is used to run the CSs. Note that, by design, the CSs should be deployed to two non-colluding servers. However, for evaluation purposes, we deployed them on the same workstation to simulate a scenario in which these two servers are in close proximity to the ESs. All servers are connected to a Gigabit network.

5.2 Benchmark Oblivious Building Blocks

Benchmark Configuration. We first evaluate four oblivious building blocks in OblivCDN (§4.3) with three metrics: computational, local I/O, and communication costs. For this benchmark, we use 2^8 5-MB videos, which can be stored by an ORAM tree with 65536 leaf nodes with 5 blocks, i.e., $\log_2 N = 17$ and $Z = 5$. To enable range access, we deployed nine ESs, with each ES dedicated to supporting

⁴<https://github.com/MonashCybersecurityLab/OblivCDN>

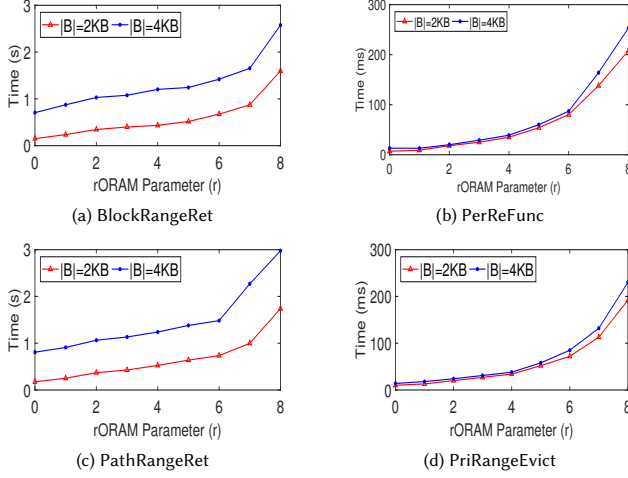


Figure 10: I/O cost of oblivious operations in the ESs.

both an E_r and S_r , where $r \in [0, 8]$. We adapted rORAM disk layout [21] to create SSD storage optimised for oblivious range access. Consequently, each E_r has 12 GB and 23 GB storage capacity when using a block size of $|B| = 2$ and 4 KB, respectively. To achieve a negligible false positive rate of 2^{-128} , we configured the fixed-size stash factor $v = 105$, so the stash size $|S_r| = 105 \times 2^r$ blocks [21]. In the CP , the *Enclave* only requires 21.05 MB to store the metadata for 2^8 videos (with around 2^{19} blocks to track).

Overall Runtime Cost. Figure 9 presents the overall cost of running four proposed oblivious building blocks. As shown in the figure, most of our oblivious operations can be completed within 20 s, except for PriRangeEvict (Figure 9d). This is because PriRangeEvict involves evicting $2^r \times \log_2 N \times Z$ blocks. Moreover, for each block eviction, both $CS_{p \in \{1,2\}}$ need to scan the entire stash. In contrast, the operations of the other building blocks work on fewer blocks, i.e., $2^r \times \log_2 N$ blocks for BlockRangeRet, and have fewer operations on blocks, i.e., each scan can permute and re-encrypt $\log_2 N \times Z$ blocks in PathRangeRet and $|S_r|$ blocks in PerReFunc.

We note that these building blocks are executed during the video upload or in the background process. Our later evaluation in §5.3 will show that they do not impact the *Subscriber*'s experience when fetching the video from the edge.

Local I/O Cost. We further dig into the I/O costs incurred by the ESs during these oblivious operations. Figure 10 shows that the I/O cost is almost negligible (< 3 s) among the overall cost.

When looking into each operation, we can see that the disk seek is still the dominant cost for the I/O. In specific, even BlockRangeRet read less blocks than PathRangeRet, i.e., $2^r \times \log_2 N$ blocks v.s. $2^r \times \log_2 N \times Z$ blocks, they incur the same I/O time because they still perform sequential seeks to all $2^r \times \log_2 N \times Z$ rORAM tree nodes. Due to the physical feature of the hard drive, the time for writing the block is faster than reading. Hence, as shown in Figure 10d, the cost of writing 2^r paths ($2^r \times \log_2 N \times Z$ blocks) in PriRangeEvict is much faster than the reading overhead of the aforementioned two building blocks. Finally, the cost of PerReFunc is the smallest among all building blocks (see Figure 10b). This is because PerReFunc only operates on S_r , which resides in volatile memory.

Table 3: Video specifications used in the evaluation.

Video Size	2 MB	127 MB	256 MB
Block Size	4 KB	256 KB	512 KB
Length/Quality	30 s/360p	5 mins/720p	5 mins/1080p

Network Communication Cost. Figure 11 shows the network communication cost with the four proposed oblivious operations when $r = 8$. It is consistent with our theoretical analysis that the CP incurs a constant and moderate (< 8 MB) inter-continental communication cost regardless of the block size and video size as it only sends instructions to the CSs.

Regarding the local region communication, we can observe a symmetric communication cost for PerReFunc and PathRangeRet since they leverage CSs to retrieve blocks from rORAM/stashes and re-route them to the stashes. For the other two operations (BlockRangeRet and PriRangeEvict), the traffic is re-shaped by DPF evaluations: In BlockRangeRet, both CSs receive $2^r \times \log_2 N$ blocks from E_r but filter out to 2^r blocks that CSs intend to reroute from the ORAM tree to the stash. Our result shows that CSs only send 1 MB (for 2 KB blocks) or 2 MB (for 4 KB blocks) to the stash even though they fetch 16.1 or 32.2 MB from the ORAM tree.

Similarly, in BlockRangeRet, both CSs receive blocks from the entire stash ($2^r \times v$ blocks) but only send a share of the targeted blocks ($2^r \times \log_2 N \times Z$ blocks) to be evicted to the ORAM tree. Since v is always larger than $\log_2 N \times Z$ to support batch fetch, this process retrieves 106 (for 2 KB blocks) and 211.4 MB (for 4 KB blocks) from the stash but only sends 50.3 and 100.2 MB to the ORAM tree. We further detail the breakdown cost under different rORAM parameters (r) in Appendix D.

5.3 Inter-continental Streaming Simulation

Streaming Setting. We replicate a real-world scenario where a *Subscriber* in Australia requests a video from a CP located in the U.S. The service provider has deployed CSs and ESs in Australia according to OblivCDN design. To simulate the intercontinental communication, we refer to real-world intercontinental delays [1] between cloud regions to introduce a 400 ms round-trip delay between CP &CSs and CP &ESs. Additionally, we put a 1 ms round-trip delay between the *Subscriber* and ESs to simulate a tiny cost incurred in the local zone [1]. Under the network setting, we test the streaming performance of three types of videos as listed in Table 3 and compare OblivCDN with the Strawman design (§3.4) and OblivP2P [55]⁵. Note that with a larger block size (256 KB and 512 KB), the rORAM with the same parameter, i.e., $\log_2 N = 17$, $Z = 5$, and $r \in [0, 8]$, can store 108 GB and 207 GB of CDN content in the ESs, respectively. Hence, our simulation can be a good illustration of the performance of streaming 180 – 345 one-hour SD (720p) videos through the Disney+ app on a mobile device *Subscriber* [69]. **Video Upload Cost.** We start with the upload cost comparison between the Strawman and OblivCDN. Note that OblivP2P is a peer-to-peer communication system with no upload phase, so we omit the comparison with OblivP2P in this part.

⁵While OblivP2P[55] and Multi-CDN [29] are compatible with real-world CDN architecture, we only pick OblivP2P for comparison, because Multi-CDN uses a different setting that relies on the collaboration between multiple *CDN providers* for privacy.

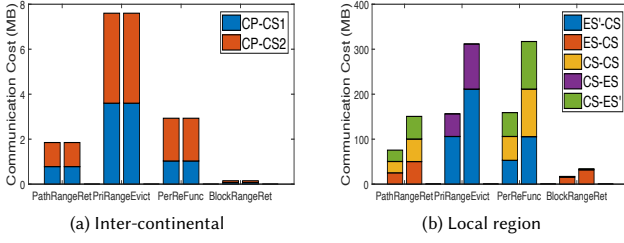


Figure 11: The communication cost (MB) of oblivious operations when $r = 8$. For each operation, the left bar is for $|B| = 2$ KB, and the right one is for $|B| = 4$ KB.

Table 4: The upload latency (s) of test videos under the Strawman and our approach, (\times): improvement.

Size	2 MB	127 MB	256 MB
Strawman	3403 (109 \times)	8356 (203 \times)	13403 (263 \times)
OblivCDN	31	41	51

Table 5: The upload communication cost (MB) of test videos under the Strawman and our approach, (\times): improvement.

Size	2 MB	127 MB	256 MB
Strawman	159.6 (7.2 \times)	10220 (69 \times)	20440 (74 \times)
OblivCDN	22	148	276

Table 6: Subscriber’s fetch latency (s), (\times): improvement

Video Size	2 MB	127 MB	256 MB
Strawman	457.9 (89 \times)	466 (87 \times)	504.4 (90 \times)
OblivP2P	16.1 (3.1 \times)	1016.9 (191.8 \times)	2050.1 (366 \times)
OblivCDN	5.1	5.3	5.6

Table 7: The background latency (s) of fetch under the Strawman and our approach, (\times): improvement.

Video Size	2 MB	127 MB	256 MB
Strawman	3403.3 (82 \times)	8355.9 (201 \times)	13403 (322 \times)
OblivCDN	41.5	41.5	41.5

During the video upload phase, the *CP* should upload a video to the targeting *ES*s. In the Strawman, *CP* conducts this task via Path ORAM operations, which involves heavy intercontinental data transfer. As shown in Table 4, the Strawman approach takes ~ 1 hour to upload a 2 MB video and almost 4 hours to upload a 256 MB one. OblivCDN significantly accelerates the process by offloading the ORAM operations to *ES*s and *CS*s. The *CP* only needs to upload all video blocks into S_r and wait for the **Sync** operation to be done. Our result shows that the upload latency for OblivCDN is at least 109 \times faster than the Strawman, as it only requires 31 s to upload the 2 MB video and 51 s for the 256 MB one.

Moreover, the Strawman design experiences communication blow-ups for large videos as it requires fetching the entire ORAM path to write one video block. Table 4 shows that it requires 80 \times more communication cost to upload the original video to the edge. In contrast, OblivCDN leverages the batch read/evict strategy to save bandwidth. The communication cost is reduced by 7.2 \times at least, and for the 256 MB video, it only sends 276 MB data to the edge, which is 74 \times smaller than that in the Strawman.

Table 8: The background communication cost (MB) of fetch under the Strawman and our approach, (\times): improvement.

Video Size	2 MB	127 MB	256 MB
Strawman	159.6 (6.1 \times)	10220 (393 \times)	20440 (786 \times)
OblivCDN	26	26	26

Table 9: Query throughput (MByte/s), (\times): improvement.

Sup. Peers	2^5	2^7	2^9
OblivP2P	0.0625 (40.6 \times)	0.25 (42.2 \times)	0.5 (84 \times)
OblivCDN	2.64	10.56	42

Video Fetch Cost. For the fetch operation, we split it into two phases, i.e., the foreground download process for *Subscribers* to obtain the requested content, and the background synchronisation process for the *CP* to instruct *CS*s to re-route the blocks.

In the first phase, the strawman approach follows the PathORAM design to scan a path and filter the targeted block in that path. On the other hand, OblivCDN follows the “read-only” ORAM design [86] to allow direct downloads on targeted blocks. As shown in Table 6, OblivCDN only requires 5.1 s to retrieve a video under the network setting. As a result, OblivCDN accelerates $\sim 90\times$ faster than the fetch process of the Strawman. OblivCDN is also much more efficient than OblivP2P (366 \times faster) since OblivP2P requires multiple peers to jointly execute the PIR scheme for each video block retrieval.

In the latter phase, OblivCDN incurs only a constant cost with given parameters, which is consistent with our theoretical analysis. In contrast, the Strawman approach imposes prohibitively high costs, as shown in Table 7 and 8. This discrepancy arises because the Strawman operates as the PathORAM client during this phase. It needs to retrieve all data blocks from the *ES* and execute the Path ORAM protocol to relocate them into new paths. Since OblivP2P does not have the background phase, we omit the comparison here. **Streaming Throughput.** In OblivCDN, each *ES* operates independently for *Subscribers* to fetch. Moreover, it minimises the blocking time of **Sync** operations as *ES* utilises another background thread to run oblivious routing protocols with *CS*s on a copy of the ORAM tree and replace the old rORAM tree with the updated one based on requests. This means if we employ more *ES*s, we can easily improve *Subscribers*’ streaming throughput via multi-thread downloading.

We subsequently conduct a streaming performance comparison with OblivP2P [55] by scaling the number of *ES*s in OblivCDN to match the number of supporting peers in OblivP2P. As shown in Table 9, we observe that OblivCDN improves 40.6 \times –84 \times query throughput compared to OblivP2P. Even with 2^5 servers, OblivCDN can effectively support the streaming of Ultra High Definition (4K UHD) videos, meeting the minimal requirement of 1.875 MBps [66].

Adaptation to multi-user concurrent accesses. The current design of *ES*s allows end-users to directly fetch entire encrypted video blocks. Hence, OblivCDN can be integrated with multi-user support systems using untrusted Load Schedulers [22, 31]. Specifically, each *ES* can work with a scheduler to group queries in a batch setting. Alternatively, an ephemeral key mechanism could be employed to support concurrent access by multiple users for the same video requests. These directions are left for future work.

6 RELATED WORKS

Access Pattern Hiding CDN Systems. Protecting content and user privacy in outsourced CDN systems is an important topic and has been widely discussed. While encryption is a straightforward solution for data confidentiality, several prior works mainly focus on the access pattern hiding feature: The first line of those works rely on anonymous routing [6], which could be prone to long-term traffic analysis [93] and may have potential copyright issues [73]. The second line focuses on fortifying users' privacy in peer-assisted CDN networks [54], which does not consider users' privacy when fetching from edge servers. The closest line of work aims to transfer CDN systems to oblivious ones with customised primitives, such as ORAM/PIR [47, 55] and queries with distributed trust [29]. However, these works are not scalable in the real-world scenario with multiple edge servers, which will multiply the bandwidth cost of the current design. Some recent works suggest having TEE-enabled devices [30, 56] for oblivious operations. These designs incur compatibility issues in CDNs with massive legacy devices.

Oblivious Query Systems. ORAMs have been widely applied in encrypted systems to ensure the obliviousness of queries. This includes searchable encryption [10, 40, 90], oblivious storage and databases [2, 7, 24, 50, 65, 79, 80, 82], and data analytic frameworks [38, 98]. We note that the adoption of ORAMs in those studies is similar to our Strawman design and will incur noticeable delays or compatibility issues under the CDN setting.

Some recent works employ the distributed trust model to enable oblivious queries. With two servers, several applications, such as ORAM storage [16, 36], data search and analytics [32, 33, 91], private messaging [37], and contact tracing [35, 87], are efficiently supported. However, those systems often duplicate the database into multiple servers' storage to support its functionality. This increases both *CDN providers'* running costs and *Subscribers'* bandwidth costs and thus makes the design not practical.

ORAM Optimisations. ORAM design has been optimised in various directions to improve computation efficiency [36, 49, 95, 97], bandwidth cost [23, 77], and query throughput [21, 22, 34, 86]. However, these works often have the eviction from a local stash to an outsourced ORAM storage. Instead, our system brings ORAM design to a practical CDN setting, which allows the eviction between both the outsourced stash and the ORAM storage deployed in *ESs*.

7 CONCLUSIONS

OblivCDN provides a novel combination of customised oblivious building blocks, range ORAM, and TEE in CDN systems to protect content confidentiality and end-user privacy from data breaches and access pattern exploitation. OblivCDN seamlessly integrates with mainstream CDNs, requiring minimal modifications. In real-world streaming evaluation, OblivCDN effectively meets CDN requirements: low user fetch latency, efficient computation, and minimal communication cost, even in intercontinental environments.

8 ACKNOWLEDGEMENTS

The authors would like to thank the anonymous reviewers for their valuable comments. This work was supported in part by the Australian Research Council Future Fellowship grant FT240100043 and a Data61-Monash Collaborative Research Project (D61 Challenge).

REFERENCES

- [1] Matt Adorjan. 2020. AWS Latency Monitoring. <https://www.cloudping.co/grid> [online]. (2020).
- [2] Adil Ahmad, Kyungtae Kim, Muhammad Ihsanulhaq Sarfaraz, and Byoungyoung Lee. 2018. OBLIVATE: A Data Oblivious Filesystem for Intel SGX. In *NDSS'18*.
- [3] Akamai. 2018. Using CDN Server Timing to Monitor CDN. <https://developer.akamai.com/blog/2018/11/16/using-cdn-server-timing-monitor-cdn-and-origin-performance>. (2018).
- [4] Akamai. 2022. Their Cloud Provider as a Competitive Threat. <https://www.akamai.com/newsroom/press-release/devops-and-the-public-cloud-the-rise-of-the-alternative-cloud>. (2022).
- [5] AWS. 2021. Confidential computing: an AWS perspective. <https://aws.amazon.com/blogs/security/confidential-computing-an-aws-perspective/>. (2021).
- [6] Michael Backes, Aniket Kate, Sebastian Meiser, and Esfandiar Mohammadi. 2014. (Nothing Else) MATor(s): Monitoring the Anonymity of Tor's Path Selection. In *CCS '14*.
- [7] Vincent Bindschadler, Muhammad Naveed, Xiaorui Pan, XiaoFeng Wang, and Yan Huang. 2015. Practicing Oblivious Access on Cloud Storage: The Gap, the Fallacy, and the New Way Forward. In *CCS'15*.
- [8] Bitdefender. 2020. Data Breach: Canada's Fitness Depot Blames ISP for Security Incident. <https://www.bitdefender.com/blog/hotforsecurity/data-breach-canadas-fitness-depot-blames-isp-for-security-incident>. (2020).
- [9] Laura Blackstone, Seny Kamara, and Tarik Moataz. 2020. Revisiting Leakage Abuse Attacks. In *NDSS'20*.
- [10] Raphael Bost, Brice Minaud, and Olga Ohrimenko. 2017. Forward and Backward Private Searchable Encryption from Constrained Cryptographic Primitives. In *ACM CCS'17*.
- [11] Thomas Bourgeat, Ilia Lebedev, Andrew Wright, Sizhuo Zhang, Arvind, and Srinivas Devadas. 2019. MI6: Secure Enclaves in a Speculative Out-of-Order Processor. In *MICRO'19*.
- [12] Elette Boyle, Niv Gilboa, and Yuval Ishai. 2015. Function Secret Sharing. In *EUROCRYPT'15*.
- [13] Elette Boyle, N. Gilboa, and Y. Ishai. 2015. Function Secret Sharing: Improvements and Extensions. In *ACM CCS'17*.
- [14] Ferdinand Brasser, Urs Müller, Alexandra Dmitrienko, Kari Kostianen, Srdjan Capkun, and Ahmad-Reza Sadeghi. 2017. Software Grand Exposure: SGX Cache Attacks Are Practical. In *WOOT'17*.
- [15] Jo Van Bulck, Nico Weichbrodt, Rüdiger Kapitza, Frank Piessens, and Raoul Strackx. 2017. Telling Your Secrets without Page Faults: Stealthy Page Table-Based Attacks on Enclaved Execution. In *USENIX Security'17*.
- [16] Paul Bunn, Jonathan Katz, Eyal Kushilevitz, and Rafail Ostrovsky. 2020. Efficient 3-Party Distributed ORAM. In *SCN'20*.
- [17] Xiang Cai, Xin Cheng Zhang, Brijesh Joshi, and Rob Johnson. 2012. Touching from a Distance: Website Fingerprinting Attacks and Defenses. In *CCS*.
- [18] David Cash, Paul Grubbs, Jason Perry, and Thomas Ristenpart. 2015. Leakage Abuse Attacks against Searchable Encryption. In *ACM CCS'15*.
- [19] Catalin Cimpanu. 2019. Data breach at Russian ISP impacts 8.7 million customers. <https://www.zdnet.com/article/data-breach-at-russian-isp-impacts-8-7-million-customers/>. (2019).
- [20] Catalin Cimpanu. 2020. Intel investigating breach after 20GB of internal documents leak online. <https://www.zdnet.com/article/intel-investigating-breach-after-20gb-of-internal-documents-leak-online/>. (2020).
- [21] Anrin Chakraborti, Adam J. Aviv, S. Choi, Travis Mayberry, Daniel S. Roche, and R. Sion. 2019. rORAM: Efficient Range ORAM with $O(\log^2 N)$ Locality. In *NDSS'19*.
- [22] Anrin Chakraborti and R. Sion. 2019. ConcurORAM: High-Throughput Stateless Parallel Multi-Client ORAM. In *NDSS'19*.
- [23] Hao Chen, Ilaria Chillotti, and Ling Ren. 2019. Onion Ring ORAM: Efficient Constant Bandwidth Oblivious RAM from (Leveled) TFHE. In *ACM CCS'19*.
- [24] Weikeng Chen and Raluca Ada Popa. 2020. Metal: A Metadata-Hiding File-Sharing System. In *NDSS'20*.
- [25] Cloudflare. 2021. Comprehensive DDoS Protection. <https://www.cloudflare.com/en-gb/ddos/>. (2021).
- [26] Cloudflare. 2021. Heartbleed Revisit. <https://blog.cloudflare.com/tag/heartbleed/>. (2021).
- [27] Cloudflare. 2021. What is a CDN? <https://www.cloudflare.com/en-au/learning/cdn/what-is-a-cdn/>. (2021).
- [28] Victor Costan and Srinivas Devadas. 2016. Intel SGX Explained. *IACR Cryptol. ePrint Arch.* (2016).
- [29] Shujie Cui, Muhammad Rizwan Asghar, and Giovanni Russello. 2020. Multi-CDN: Towards Privacy in Content Delivery Networks. *IEEE TDSC* (2020).
- [30] Simon Da Silva, Sonia Ben Mokhtar, Stefan Contiu, Daniel Nègru, Laurent Réveillère, and Etienne Rivière. 2019. PrivaTube: Privacy-Preserving Edge-Assisted Video Streaming. In *Middleware '19*.
- [31] Emma Dauterman, Vivian Fang, Ioannis Demertzis, Natacha Crooks, and Raluca Ada Popa. 2021. Snoopy: Surpassing the Scalability Bottleneck of Oblivious Storage. In *SOSP '21*.

- [32] Emma Dauterman, Eric Feng, Ellen Luo, Raluca A. Popa, and Ion Stoica. 2020. DORY: An Encrypted Search System with Distributed Trust. In *OSDI'20*.
- [33] Emma Dauterman, Mayank Rathee, Raluca A. Popa, and Ion Stoica. 2022. Waldo: A Private Time-Series Database from Function Secret Sharing. In *IEEE S&P'22*.
- [34] Ioannis Demertzis and Charalampos Papamanthou. 2017. Fast Searchable Encryption with Tunable Locality. In *ACM SIGMOD'17*.
- [35] Samuel J. Dittmer, Yuval Ishai, Steve Lu, Rafail Ostrovsky, Mohamed Elsabagh, Nikolaos Kiourtis, Brian Schulte, and Angelos Stavrou. 2020. Function Secret Sharing for PSI-CA: With Applications to Private Contact Tracing. *ArXiv abs/2012.13053* (2020).
- [36] Jack Doerner and Abhi Shelat. 2017. Scaling ORAM for Secure Computation. In *ACM CCS'17*.
- [37] Saba Eskandarian, Henry Corrigan-Gibbs, Matei A. Zaharia, and Dan Boneh. 2021. Express: Lowering the Cost of Metadata-hiding Communication with Cryptographic Privacy. In *USENIX Security'21*.
- [38] Saba Eskandarian and Matei Zaharia. 2019. OblIDB: Oblivious Query Processing for Secure Databases. *Proc. VLDB Endow.* (2019).
- [39] Andriy Panchenko et al. 2016. Website Fingerprinting at Internet Scale. In *NDSS*.
- [40] Javad Ghareh Chamani, Dimitrios Papadopoulos, Charalampos Papamanthou, and Rasool Jalili. 2018. New Constructions for Forward and Backward Private Symmetric Searchable Encryption. In *ACM CCS'18*.
- [41] Y. Gilad, A. Herzberg, Michael Sudkovitch, and Michael Gopherman. 2016. CDN-Demand: An affordable DDoS Defense via Untrusted Clouds. In *NDSS'16*.
- [42] Niv Gilboa and Yuval Ishai. 2014. Distributed Point Functions and Their Applications. In *EUROCRYPT'14*.
- [43] GlobalDots. 2022. CDN Logs. <https://www.globaldots.com/resources/blog/cdn-logs-are-priceless-how-can-you-better-use-them/>. (2022).
- [44] Johannes Götzfried, Moritz Eckert, Sebastian Schinzel, and Tilo Müller. 2017. Cache Attacks on Intel SGX. In *EuroSec'17*.
- [45] Daniel Gruss, Julian Lettner, Felix Schuster, Olga Ohrimenko, Istvan Haller, and Manuel Costa. 2017. Strong and Efficient Cache Side-channel Protection Using Hardware Transactional Memory. In *USENIX Security'17*.
- [46] Run Guo, Weizhong Li, Baojun Liu, S. Hao, Jia Zhang, Haixin Duan, Kaiwen Sheng, Jianjun Chen, and Y. Liu. 2020. CDN Judo: Breaking the CDN DoS Protection with Itself. In *NDSS'20*.
- [47] Trinabh Gupta, Natacha Crooks, Whitney Mulhern, Srinath Setty, Lorenzo Alvisi, and Michael Walfish. 2016. Scalable and Private Media Consumption with Popcorn. In *NSDI'16*.
- [48] Stephen Herwig, Christina Garman, and Dave Levin. 2020. Achieving Keyless CDNs with Conclaves. In *USENIX Security'20*.
- [49] Thang Hoang, Jorge Guajardo, and Attila Yavuz. 2020. MACAO: A Maliciously-Secure and Client-Efficient Active ORAM Framework. In *NDSS'20*.
- [50] Thang Hoang, Muslum Ozgur Ozmen, Yeongjin Jang, and Attila A. Yavuz. 2019. Hardware-Supported ORAM in Effect: Practical Oblivious Search and Update on Very Large Dataset. In *PET'19*.
- [51] Intel. 2021. Tangible Results for Content Delivery Networks. <https://www.intel.com/content/dam/www/public/us/en/documents/faqs/visual-cloud-tangible-results-faq.pdf>. (2021).
- [52] M Islam, Mehmet Kuzu, and Murat Kantarcioglu. 2012. Access pattern disclosure on searchable encryption: Ramification, attack and mitigation. In *NDSS'12*.
- [53] Jaikumar Vijayan. 2007. Pfizer Breach Exposes Data. <https://www.computerworld.com/article/2552147/pfizer-breach-exposes-data-on-34-000-people.html>. (2007).
- [54] Yaoqi Jia, Guangdong Bai, Prateek Saxena, and Zhenkai Liang. 2016. Anonymity in Peer-assisted CDNs: Inference Attacks and Mitigation. In *PET'16*.
- [55] Yaoqi Jia, Tarik Moataz, Shruti Tople, and P. Saxena. 2016. OblivP2P: An Oblivious Peer-to-Peer Content Sharing System. In *USENIX Security'16*.
- [56] Yaoqi Jia, Shruti Tople, Tarik Moataz, Deli Gong, P. Saxena, and Zhenkai Liang. 2020. Robust Synchronous P2P Primitives Using SGX Enclaves. In *RAID'20*.
- [57] Seny Kamara and Tarik Moataz. 2019. Computationally Volume-Hiding Structured Encryption. In *EUROCRYPT'19*.
- [58] Seny Kamara, Payman Mohassel, and Mariana Raykova. 2011. Outsourcing Multi-Party Computation. *Cryptology ePrint Archive, Report 2011/272*. (2011).
- [59] Shangqi Lai, Xingliang Yuan, Joseph K. Liu, X. Yi, Qi Li, D. Liu, and S. Nepal. 2021. OblivSketch: Oblivious Network Measurement as a Cloud Service. In *NDSS'21*.
- [60] Dayeol Lee, David Kohlbrenner, Shweta Shinde, Krste Asanović, and Dawn Song. 2020. Keystone: An Open Framework for Architecting Trusted Execution Environments. In *EuroSys'20*.
- [61] Jaehyuk Lee, Jinsoo Jang, Yeongjin Jang, Nohyun Kwak, Yeseul Choi, Changho Choi, Taesoo Kim, Marcus Peinado, and Brent Byunghoon Kang. 2017. Hacking in Darkness: Return-Oriented Programming against Secure Enclaves. In *USENIX Security'17*.
- [62] Sangho Lee, Ming-Wei Shih, Prasun Gera, Taesoo Kim, Hyesoon Kim, and Marcus Peinado. 2017. Inferring Fine-grained Control Flow Inside SGX Enclaves with Branch Shadowing. In *USENIX Security'17*.
- [63] Microsoft. [n. d.]. Microsoft Azure. <https://azure.microsoft.com/en-us/solutions/confidential-compute/>. ([n. d.]).
- [64] Microsoft. 2018. Mitigating hardware Vulnerabilities. <https://msrc-blog.microsoft.com/2018/03/15/>. (2018).
- [65] P. Mishra, R. Poddar, J. Chen, A. Chiesa, and R. A. Popa. 2018. Obliv: An Efficient Oblivious Search Index. In *IEEE S&P'18*.
- [66] Netflix. [n. d.]. Internet connection speed recommendations. <https://help.netflix.com/en/node/306>. ([n. d.]).
- [67] Netflix. 2016. Completing the Netflix Cloud Migration. <https://about.netflix.com/en/news/completing-the-netflix-cloud-migration>. (2016).
- [68] Netflix. 2019. Open Connect. <https://openconnect.netflix.com/>. (2019).
- [69] Netflix. 2021. Data usage and streaming quality on Disney+. https://help.disneyplus.com/csp?id=csp_article_content&sys_kb_id=5e43f0cfdb7fb018db5ed404ca96192c. (2021).
- [70] Netflix. 2021. Disabling appliances for maintenance. <https://openconnect.zendesk.com/hc/en-us/articles/115001068772>. (2021).
- [71] Netflix. 2021. Netflix Open Connect Operating Level Agreement. <https://openconnect.netflix.com/ola.pdf>. (2021).
- [72] Netflix. 2021. Netflix Works With ISPs Around the Globe. <https://about.netflix.com/en/news/how-netflix-works-with-isps-around-the-globe-to-deliver-a-great-viewing-experience>. (2021).
- [73] Netflix. 2022. Netflix says 'You seem to be using a VPN or proxy.'. <https://help.netflix.com/en/node/277>. (2022).
- [74] Olga Ohrimenko, Felix Schuster, Cédric Fournet, Aastha Mehta, Sebastian Nowozin, Kapil Vaswani, and Manuel Costa. 2016. Oblivious Multi-Party Machine Learning on Trusted Processors. In *USENIX Security'16*.
- [75] Rishabh Poddar, Ganesh Ananthanarayanan, Srinath Setty, Stavros Volos, and Raluca Ada Popa. 2020. Revisiting Leakage Abuse Attacks. In *USENIX Security'21*.
- [76] A. Rane, C. Lin, and Mohit Tiwari. 2015. Raccoon: Closing Digital Side-Channels through Obfuscated Execution. In *USENIX Security'15*.
- [77] Ling Ren, Christopher Fletcher, Albert Kwon, Emil Stefanov, Elaine Shi, Marten van Dijk, and Srinivas Devadas. 2015. Constants Count: Practical Improvements to Oblivious RAM. In *USENIX Security'15*.
- [78] Research and Markets. 2021. CDN Market. <https://www.researchandmarkets.com/reports/5401912/cdn-market-by-technology-platform-application>. (2021).
- [79] Cetin Sahin, Victor Zakhary, Amr El Abbadi, Huijia Lin, and Stefano Tessaro. 2016. TaoStore: Overcoming Asynchronicity in Oblivious Data Storage. In *IEEE S&P'16*.
- [80] Sajin Sasy, Sergey Gorbunov, and Christopher W. Fletcher. 2017. ZeroTrace: Oblivious Memory Primitives from Intel SGX. In *NDSS'17*.
- [81] Roei Schuster, Vitaly Shmatikov, and Eran Tromer. 2017. Beauty and the Burst: Remote Identification of Encrypted Video Streams. In *USENIX Security'17*.
- [82] Elaine Shi. 2020. Path Oblivious Heap: Optimal and Practical Oblivious Priority Queue. In *IEEE S&P'20*.
- [83] Emil Stefanov, Marten van Dijk, Elaine Shi, T-H. Hubert Chan, Christopher Fletcher, Ling Ren, et al. 2013. Path ORAM: An Extremely Simple Oblivious RAM Protocol. In *ACM CCS'13*.
- [84] Thales Group. 2022. 2022 Thales Cloud Security Study. <https://cpl.thalesgroup.com/cloud-security-research>. (2022).
- [85] The Integrity360 Team. 2019. The Adverline Breach and the Emerging Risk of Using Third-Party Vendors. (2019). <https://insights.integrity360.com/the-adverline-breach>
- [86] S. Tople, Y. Jia, and P. Saxena. 2019. {PRO-ORAM}: Practical {Read-Only} Oblivious {RAM}. In *RAID'19*.
- [87] Ni Trieu, Kareem Shehata, P. Saxena, R. Shokri, and Dawn Xiaodong Song. 2020. Epione: Lightweight Contact Tracing with Strong Privacy. *ArXiv abs/2004.13293* (2020).
- [88] UpGuard. 2019. Out of Pocket: How an ISP Exposed Administrative System Credentials. <https://www.upguard.com/breaches/out-of-pocket-how-an-isp-exposed-administrative-system-credentials>. (2019).
- [89] Jo Van Bulck, Marina Minkin, Ofir Weisse, Daniel Genkin, Baris Kasikci, Frank Piessens, Mark Silberstein, Thomas F. Wenisch, Yuval Yarom, and Raoul Strackx. 2018. Foreshadow: Extracting the Keys to the Intel SGX Kingdom with Transient out-of-Order Execution. In *USENIX Security'18*.
- [90] Viet Vo, Shangqi Lai, Xingliang Yuan, Shi-Feng Sun, Surya Nepal, and Joseph K. Liu. 2020. Accelerating Forward and Backward Private Searchable Encryption Using Trusted Execution. In *ACNS'20*.
- [91] Frank Wang, Catherine Yun, Shaif Vaikuntanathan, and Matei Zaharia. 2017. Splinter: Practical Private Queries on Public Data. In *NSDI'17*.
- [92] Kailong Wang, Junzhe Zhang, Guangdong Bai, Ryan Ko, and Jin Song Dong. 2021. It's Not Just the Site, It's the Contents: Intra-Domain Fingerprinting Social Media Websites Through CDN Bursts. In *WWW'21*.
- [93] Tao Wang, Xiang Cai, Rishabh Nithyanand, Rob Johnson, and Ian Goldberg. 2014. Effective Attacks and Provable Defenses for Website Fingerprinting. In *USENIX Security'14*.
- [94] Wenhao Wang, Guoxing Chen, Xiaorui Pan, Yinqian Zhang, Xiaofeng Wang, Vincent Bindshaedler, Haixu Tang, and Carl A. Gunter. 2017. Leaky Cauldron on the Dark Land: Understanding Memory Side-Channel Hazards in SGX. In *ACM CCS'17*.

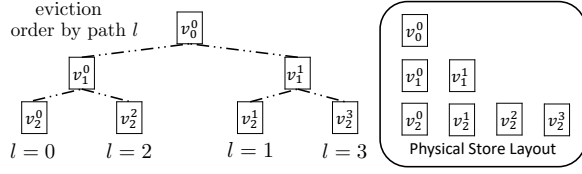


Figure 12: rORAM physical and logical storage layout.

- [95] Xiao Wang, Hubert Chan, and Elaine Shi. 2015. Circuit ORAM: On Tightness of the Goldreich-Ostrovsky Lower Bound. In *ACM CCS'15*.
- [96] Y. Xu, W. Cui, and M. Peinado. 2015. Controlled-Channel Attacks: Deterministic Side Channels for Untrusted Operating Systems. In *IEEE S&P'15*.
- [97] Samee Zahur, Xiao Wang, Mariana Raykova, Adrià Gascón, Jack Doerner, David Evans, and Jonathan Katz. 2016. Revisiting Square-Root ORAM: Efficient Random Access in Multi-party Computation. In *IEEE S&P'16*.
- [98] Wenting Zheng, Ankur Dave, Jethro G. Beekman, Raluca A. Popa, Joseph E. Gonzalez, and Ion Stoica. 2017. Opaque: An Oblivious and Encrypted Distributed Analytics Platform. In *NSDI'17*.

A rORAM PROTOCOL

Let N be the number of blocks in an ORAM storage with the height L , and $\text{bid}_{i \in [0, N]}$ be the identifier of a block, and R be the largest sequence of blocks allowed to fetch each time from storage. The rORAM scheme [22] consists of $\log_2 R + 1$ ORAM storage deployed at the server side, denoted as E_r , where $r \in [0, \log_2 R]$. The client maintains the corresponding S_r and a position map position_r .

A unique design for rORAM is that it partitions the server's disk to store each layer of the ORAM tree in consecutive physical space (see the right part of Figure 12) but arrange them in a bit-reversed order, which means the paths are encoded as 0(00), 2(10), 1(01), 3(11) in a three-layer ORAM tree (the left part of Figure 12). The above design enables sequential accesses on consecutive paths and minimises the overlapping between consecutive paths to mitigate overflow when evicting blocks. For instance, when accessing the path 0, 1, 2, the rORAM client can sequentially access v_0^0, v_0^0, v_0^0 on layer 0, v_1^0, v_1^1, v_1^0 on layer 1 and v_2^0, v_2^1, v_2^2 on layer 2 to finalise the access, which only requires $O(\log_2 N)$ seeks. The eviction on those paths are following the same process but in a bottom-up order, which also indicates $O(\log_2 N)$ seeks.

Furthermore, rORAM realises a location-sensitive mapping strategy to assign bids and paths to blocks. In particular, to store 2^r blocks into E_r , the rORAM client assigns a random bid and path l to the starting block, and then assigns $\text{bid} + i$ and $(l + i) \bmod 2^{(L-1)}$ for $i \in [1, 2^r)$ to the following blocks. By doing this, rORAM ensures that for blocks that belong to the same range, they are always in consecutive paths, and thus store close to each other to maintain minimised seek cost $O(\log_2 N)$. For blocks that are not in the same range, the ORAM randomisation strategy is still in place to ensure the full obliviousness. At the end, we provide the detailed rORAM protocols as in Algorithm 2 and 3.

B ALGORITHMS OF BUILDING BLOCKS

In this section, we present the set of building blocks used to build the system in §4. In general, we denote G as pseudo random function we used in this paper.

Algorithm 2 $E_r.\text{ReadRange}(\text{bid})$

```

1: Let  $U := [\text{bid}, \text{bid} + 2^r)$ 
2: Scan  $S_r$  for blocks in the range  $U$ .
3:  $p \leftarrow \text{position}_r.\text{query}(\text{bid})$   $\triangleright$  get the ORAM path  $p$  for the block  $\text{bid}$ .
4: for  $e = 0, \dots, L - 1$  do
5:   Read ORAM buckets  $V = \{v_e^t \bmod 2^e : t \in [p, p + 2^r)\}$ 
6:   Identify blocks of  $U$  from  $V$ .
7: end for
8:  $p' \leftarrow [0, N)$   $\triangleright$  identify a new random path
9:  $\text{position}_r.\text{update}(\text{bid} + i, p' + i)$  for  $i \in [0, 2^r)$ , wrap around  $N$ .

```

Algorithm 3 $E_r.\text{BatchEvict}(k)$

```

1: Let  $G_r$  be an integer tracking the eviction schedule of  $E_r$ 
2: for  $e = 0, \dots, L - 1$  do  $\triangleright$  fetch blocks on  $k$  paths
3:   Read ORAM buckets  $V = \{v_e^t \bmod 2^e : t \in [G_r, G_r + k)\}$ 
4:   Put not-dummy blocks in  $V$  to  $S_r$ 
5: end for
6: for  $e = L - 1, \dots, 0$  do  $\triangleright$  evict  $k$  paths: bottom-up, level-by-level
7:   for  $i \in \{t \bmod 2^e : t \in [G_r, G_r + k)\}$  do  $\triangleright$  for each path
8:      $\triangleright$  Let  $l_j$  be the current ORAM path of the block  $j$ 
9:      $S' \leftarrow \{\text{block}_j \in S_r : l_j \equiv i \pmod{2^e}\}$ 
10:     $S' \leftarrow \text{Select min}(|S'|, Z)$  blocks from  $S'$ 
11:     $S_r \leftarrow S_r / S'$ 
12:     $\triangleright$  Let  $v_e^i \bmod 2^e$  be the partition  $e$  with offset  $(i \bmod 2^e)$ 
13:     $v_e^i \bmod 2^e \leftarrow S'$   $\triangleright$  note the starting offset to write  $S'$  at  $e$ 
14:   end for
15: end for
16: for  $e = 0, \dots, L - 1$  do
17:   Write ORAM buckets  $\{v_e^t \bmod 2^e : t \in [G_r, G_r + k)\}$  to  $E_r$ 
18: end for

```

<p>$\text{OGet}(S, k) :$</p> <pre> 1: $v \leftarrow \perp$ 2: for $i = 0$ to $S - 1$ do 3: $c \leftarrow \text{ocmp}(i, k)$ 4: $\text{ouupdate}(c, S[i], v)$ 5: return v </pre>	<p>$\text{OUpdate}(S, k, v) :$</p> <pre> 1: for $i = 0$ to $S - 1$ do 2: $c \leftarrow \text{ocmp}(i, k)$ 3: $\text{ouupdate}(c, v, S[i])$ </pre>
---	--

Figure 13: OGet and OUpdate

B.1 Oblivious Functions in the Enclave

Many techniques have been proposed to mitigate memory access side-channel attacks [14, 15, 62, 94] by obfuscating the access of the *Enclave* to CPU's caches [74, 76, 80]. Figure 13 demonstrates common oblivious functions, i.e., OGet and OUpdate, that enable the *Enclave* to *obliviously* access the vector, including the stash in VideoMap, BlockStateMap, and the Strawman design). Note that **ouupdate** (i.e., oblivious update) and **ocmp** (i.e., oblivious comparison) are constructed based on CMOV and SETE instructions.

B.2 Block Range Return

BlockRangeRet enables routing a collection of 2^r video blocks from the ORAM storage E_r to the S_r (Algorithm 4).

Let Q be the range query collection, where each block b_{s_i} , identified by bid_i , with block state (c_i, l_i, s_i) . The algorithm re-encrypts

Algorithm 4 BlockRangeRet(Q)

Require: Query List $Q = \{(bid_i, c_i, l_i, l'_i, s_i, s'_i)\}$, where $i \in [a, a + 2^r]$

- 1: **Inside the Enclave:**
- 2: Init query batches Q_1 and Q_2
- 3: **for** $(bid_i, c_i, l_i, s_i, s'_i) \in Q$ **do** ▷ generate instructions
- 4: $(k_{i,1}, k_{i,2}) \leftarrow \text{DPF.Gen}(1^\lambda, s_i)$
- 5: $m_{i,1} \xleftarrow{\$} (0, 1)^\lambda$
- 6: $m_{i,2} \leftarrow m_{i,1} \oplus G(c_i) \oplus G(c_i + 1)$
- 7: $o_i \leftarrow (s_i - |S_r|) \% Z$
- 8: $Q_1 \leftarrow Q_1 \cup \{(k_{i,1}, m_{i,1}, l_i, o_i, s'_i)\}$
- 9: $Q_2 \leftarrow Q_2 \cup \{(k_{i,2}, m_{i,2}, l_i, o_i, s'_i)\}$
- 10: Oblivious update BlockState[bid_i] with $(c_i + 1)$, l'_i and s'_i
- 11: **end for**
- 12: Enclave sends Q_p to CS_p , $p \in \{1, 2\}$.
- 13: **On each** CS_p , $p \in [1, 2]$:
- 14: **for** $i \in [a, a + 2^i]$ **do** ▷ convert instructions to oblivious operations
- 15: **for** $e \in [1, \log_2 N]$ **do** ▷ on each layer of E_r
- 16: Compute target block ID $s_e = |S_r| + (e - 1) \times N + o_i$
- 17: Retrieve block b_{s_e} at the offset o_i of the e level of path l_i inside E_r
- 18: $y_{i,p}^e \leftarrow \text{Eval}(k_{i,p}, s_e)$
- 19: **end for**
- 20: $b_{i,p} \leftarrow \bigoplus_{e=1}^{\log_2 N} (y_{i,p}^e \times b_{s_e})$
- 21: Send $b_{i,p} \leftarrow (b_{i,p} \oplus m_{i,p})$ and s'_i to S_r
- 22: **end for**
- 23: **On** S_r :
- 24: **for** $i \in [a, a + 2^i]$ **do** ▷ Update on S_r
- 25: Store $(b_{i,1} \oplus b_{i,2})$ at s'_i of S_r
- 26: **end for**

b_{s_i} with new counter $c_i + 1$ and places the re-encrypted versions of the block in a randomly selected s'_i index in the S_r . and its block state is updated accordingly.

B.3 Permutation & Re-encryption

PerReFunc re-encrypts and shuffles all blocks in the S_r , which is presented in Algorithm 5.

The *Enclave* in the *CP* triggers PerReFunc by permuting the MetaStash $_r$ via the mapping ω that indicates new random location and re-encrypted block for every block within the S_r . Then, ω and re-encryption keys are then shared to each $CP_p \in \{1, 2\}$. In this way, each of them cannot determine the re-encryption keys or trace the location replacement of blocks in the S_r .

B.4 Path Range Return

Algorithm 6 details PathRangeRet. Given the set Q which contains blocks in 2^r ORAM paths of an ORAM storage E_r , the PathRangeRet allows the *CP* to route them to *ESs* that maintains the S_r . For each block bid_i in Q , the *Enclave* generates the random permutation ω and re-encryption keys that can be shared to *CSs*. The path information is given, so CS_1 and CS_2 can correctly fetch, re-encrypt and permute the blocks according to the instruction. But throughout the process, CS_1 will only know where the block comes from while CS_2 knows where the block will be stored in the S_r .

B.5 Private Range Eviction

Given the set Q , the collection of $2^r \times \log_2 N \times Z$ blocks currently located in the S_r , the PriRangeEvict privately writes them to 2^r ORAM paths in the storage E_r .

Let a block i , with bid_i and the current state c_i , is located at the index s_i in the S_r . PriRangeEvict privately route the block to the

Algorithm 5 PerReFunc(Q)

Require: Query List $Q = \{(bid_i, s_i, s'_i)\}$, where $i \in [0, |S_r|]$

- 1: **Inside the Enclave:**
- 2: Init query batches Q_1 and Q_2
- 3: **for** $(bid_i, s_i, s'_i) \in Q$ **do** ▷ generate instructions
- 4: Sample a permutation $\omega_{i,1} : s_i \mapsto s_i^*, \omega_{i,2} : s_i^* \mapsto s'_i$
- 5: $m_{i,1} \xleftarrow{\$} (0, 1)^\lambda$
- 6: $m_{i,2} \leftarrow m_{i,1} \oplus G(c_i) \oplus G(c_i + 1)$
- 7: $Q_1 \leftarrow Q_1 \cup \{(\omega_{i,1}, m_{i,1})\}$
- 8: $Q_2 \leftarrow Q_2 \cup \{(\omega_{i,2}, m_{i,2})\}$
- 9: Oblivious update BlockState[bid_i] with $(c_i + 1)$ and s'_i
- 10: **end for**
- 11: Enclave sends Q_p to CS_p , $p \in \{1, 2\}$.
- 12: **On** CS_1 :
- 13: **for** $s \in [0, |S_r|]$ **do**
- 14: Retrieve block b_s from S_r
- 15: Compute $b_s \leftarrow b_s \oplus m_{s,1}$
- 16: Permute b_s with $\omega_{s,1}$
- 17: **end for**
- 18: Send permuted blocks to CS_2 in order
- 19: **On** CS_2 :
- 20: **for** $s \in [0, |S_r|]$ **do**
- 21: Received block b_s from CS_1
- 22: Compute $b_s \leftarrow b_s \oplus m_{s,2}$
- 23: Permute b_s with $\omega_{s,2}$
- 24: **end for**
- 25: Store permuted blocks back to S_r in order

Algorithm 6 PathRangeRet(Q)

Require: Query List $Q = \{(bid_i, l_i, s_i, s'_i)\}$, where $i \in [0, 2^r \times \log_2 N \times Z]$

- 1: **Inside the Enclave:**
- 2: Init query batches Q_1 and Q_2
- 3: **for** $(bid_i, l_i, s_i, s'_i) \in Q$ **do** ▷ generate instructions
- 4: Sample a permutation $\omega_{i,1} : s_i \mapsto s_i^*, \omega_{i,2} : s_i^* \mapsto s'_i$
- 5: $m_{i,1} \xleftarrow{\$} (0, 1)^\lambda$
- 6: $m_{i,2} \leftarrow m_{i,1} \oplus G(c_i) \oplus G(c_i + 1)$
- 7: $Q_1 \leftarrow Q_1 \cup \{(l_i, \omega_{i,1}, m_{i,1})\}$
- 8: $Q_2 \leftarrow Q_2 \cup \{(l_i, \omega_{i,2}, m_{i,2})\}$
- 9: Oblivious update BlockState[bid_i] with $(c_i + 1)$ and s'_i
- 10: **end for**
- 11: Enclave sends Q_p to CS_p , $p \in \{1, 2\}$.
- 12: **On** CS_1 :
- 13: **for each instruction** $\{(l_i, \omega_{i,1}, m_{i,1})\}$ in Q_1 **do**
- 14: Retrieve block b_{s_i} from path l_i of E_r
- 15: Compute $b_{s_i} \leftarrow b_{s_i} \oplus m_{s_i,1}$
- 16: Permute b_{s_i} with $\omega_{s_i,1}$
- 17: **end for**
- 18: Send permuted blocks to CS_2 in order
- 19: **On** CS_2 :
- 20: **for each instruction** $\{l_i, \omega_{i,1}, m_{i,1}\}$ in Q_2 **do**
- 21: Retrieve block b_{s_i} of path l_i from CS_1
- 22: Compute $b_{s_i} \leftarrow b_{s_i} \oplus m_{s_i,2}$
- 23: Permute b_{s_i} with $\omega_{s_i,2}$
- 24: **end for**
- 25: Store permuted blocks back to S_r in order

location s'_i in E_r . Algorithm 7 presents this building block. Note that s'_i can be easily converted to layer and offset information that can be used to uniformly locate a block with path information l_i .

C SECURITY ANALYSIS**C.1 Overview**

As mentioned, in OblivCDN, we follow real-world CDN systems [67, 68] to consider four parties, i.e., the *CDN service provider*, the *cloud service providers*, the *ISP partners*, and the *Subscriber*, where the *cloud service providers* and *ISP partners* are considered as untrusted. Hence, the security analysis will start from the most simple case,

Algorithm 7 PriRangeEvict(Q)

Require: Query List $Q = \{(bid_i, c_i, l_i, l'_i, s_i, s'_i)\}$, where $i \in [a, a+2^r \times \log_2 N \times Z]$

- 1: **Inside the Enclave:**
- 2: Init query batches Q_1 and Q_2
- 3: **for** $(bid_i, c_i, l_i, s_i, s'_i) \in Q$ **do** ▷ generate instructions
- 4: $(k_{i,1}, k_{i,2}) \leftarrow \text{DPF.Gen}(1^\lambda, s_i)$
- 5: $m_{i,1} \xleftarrow{\$} (0, 1)^\lambda$
- 6: $m_{i,2} \leftarrow m_{i,1} \oplus G(c_i) \oplus G(c_i + 1)$ if $bid_i \neq -1$; otherwise, $k_{i,2} \xleftarrow{\$} (0, 1)^\lambda$
- 7: $Q_1 \leftarrow Q_1 \cup \{(k_{i,1}, m_{i,1}, l_i, s'_i)\}$
- 8: $Q_2 \leftarrow Q_2 \cup \{(k_{i,2}, m_{i,2}, l_i, s'_i)\}$
- 9: Oblivious update BlockState[bid_i] with $(c_i + 1)$ and s'_i
- 10: **end for**
- 11: Enclave sends Q_p to CS_p , $p \in \{1, 2\}$
- 12: **On each** CS_p , $p \in [1, 2]$:
- 13: Retrieve the entire S_r with block $b_{s,s} \in [0, |S_r|]$
- 14: **for** each instruction $(k_{i,p}, m_{i,p}, l_i, s'_i)$ in Q_p **do** ▷ convert instructions to oblivious operations
- 15: **for** $s \in [0, |S_r|]$ **do**
- 16: $y_{i,p}^s \leftarrow \text{Eval}(k_{i,p}, s)$
- 17: **end for**
- 18: $b_{i,p} \leftarrow \bigoplus_{s=0}^{|S_r|-1} (y_{i,p}^s \times b_s)$
- 19: **end for**
- 20: Send $b_{i,p} \leftarrow (b_{i,p} \oplus m_{i,p})$ and (l_i, s'_i) to E_r
- 21: **On** E_r :
- 22: **for** $i \in [a, a + 2^r \times \log_2 N \times Z]$ **do** ▷ Update on E_r
- 23: Compute $e_i \leftarrow \lfloor (s'_i - |S_r|) / Z \rfloor + 1$ and offset $o_i \leftarrow (s'_i - |S_r|) \% Z$
- 24: Store $(b_{i,1} \oplus b_{i,2})$ at offset o_i of the layer e_i of path l_i on E_r
- 25: **end for**

where the *CDN service provider* leverages three distinct *cloud service providers* to deploy CP , CS_1 , and CS_2 , respectively. And for the *ISP partner*, the *CDN service provider* is contracted with an *ISP partner* to host all ES s. In the above model, it clear that each party can only observe the local view for the entire OblivCDN system, and we will depict the view of those parties and demonstrate their security guarantees under the real/ideal paradigm.

Then, we will discuss more realistic cases with bandwidth-saving and economical considerations: The first case is that the *CDN service provider* deploys one CS on the *ISP partner* who hosts ES s, which will further enable the *ISP partner* to collect information from CS . The second one, on the top of the first case, further considers the *CDN service provider* to use the servers from the same *cloud service provider* but located in different regions (e.g., AWS instances in multiple available zones) to deploy CP and another CS , respectively. This enables the *cloud service provider* to collect the information both from CP and one CS . Our goal is to illustrate that even OblivCDN contains some servers controlled by the same concerned party, its security guarantee will not be compromised if *cloud service providers* and *ISP partners* are not colluding.

C.2 Primitive Security

PRF/PRP Security. Both pseudorandom functions (PRFs) and pseudorandom permutations (PRPs) can be considered as indistinguishable from the random functions to adversaries [?], In the following sections, we use random functions to replace PRFs/PRPs, while the adversary only has a negligible chance to distinguish them.

ORAM Security. The ORAM security ensures that any access request sequences with the same length always result the an indistinguishable access pattern. The only thing can be observe is the statistical information regarding the ORAM store, which is the

number of tree nodes N , the number of blocks in each node Z , and the block size B for Path ORAM [83]. Meanwhile, the rORAM additionally reveals the maximum supported range R , and range size 2^r , $r \in [0, \log_2 R]$ supported by each ORAM tree [21]. A simulator for Path ORAM (S_{ORAM}) and rORAM (S_{rORAM}) can use the above-mentioned statistical information to initialise and simulate random access pattern accordingly without losing its correctness. **TEE Security.** For TEE, it provides an isolated memory region (called Enclave) in a server that cannot be directly read by other parts that are considered as untrusted. Furthermore, all data loaded into the Enclave will be automatically encrypted and only decrypted when loaded and processing inside CPU [28]. However, adversaries can use side-channels [14, 44, 45, 96] to extract the access pattern of that isolated memory region even they cannot read the memory or decrypt its content.

DPF Security. DPF guarantees that the primitive leaks no information regarding the input x^* and $f(x)$ to the corrupted party [13]. Formally, given the point function f , the leakage function of DPF regarding f can be defined as $\mathcal{L}_{\text{DPF}}(f) = (l, \mathbb{F})$, where l is the input size, and \mathbb{F} is f 's output field. The simulator S_{DPF} takes the security parameter λ and $\mathcal{L}_{\text{DPF}}(f)$ as inputs to simulate DPF keys. The simulated keys are indistinguishable from the keys generated by the real DPF instantiation, while maintaining DPF's correctness.

C.3 Security Definition for OblivCDN Entities

We start from the security definition of each individual entities of OblivCDN. For the adversaries on CP , denoted as \mathcal{A}_{CP} , its view can be defined as the Path ORAM/rORAM parameters (i.e., N, Z, B, R, r), which can be extracted from the access pattern on allocated location even it is inside the *Enclave*. Nonetheless, the above leaked information will not have any negative impact on the data-oblivious guarantee to the *Subscriber* as stated in the following theorem:

THEOREM 1. *Let Π be the scheme of (Setup, Upload, Fetch, Sync). The adversary on CP (\mathcal{A}_{CP}) chooses the Path ORAM and rORAM parameters (N, Z, B, R) for Setup and selects a list of same-length videos for the *CDN service provider* to Upload. Later, \mathcal{A}_{CP} can arbitrarily Fetch videos and observe the access pattern on CP . OblivCDN ensures that the Enclave in the CP is data-oblivious, assuming that Path ORAM and rORAM are data-oblivious, the PRF construction is secure, the permutations are selected uniformly at random, and TEE isolation and encryption features are available.*

Similarly, we can define the adversary on one of $CS_{p \in \{1,2\}}$ (\mathcal{A}_{CS_p}), who also chooses the Path ORAM and rORAM parameters, as well as a list of same-length videos for Upload and Fetch. However, we claim that adversaries can only learn the ORAM parameters if they only compromise one CS :

THEOREM 2. *Let Π be the scheme of (Setup, Upload, Fetch, Sync). The adversary on $CS_{p \in \{1,2\}}$ (\mathcal{A}_{CS_p}) chooses the Path ORAM and rORAM parameters (N, Z, B, R) for Setup and selects a list of same-length videos for the *CDN service provider* to Upload. Later, \mathcal{A}_{CS_p} can arbitrarily Fetch videos and observe the tokens and blocks sent in and out on CS_p . OblivCDN ensures that CS is data-oblivious against the adversary, assuming that rORAM is data-oblivious, the DPF and PRF constructions are secure, and the permutations are selected uniformly at random.*

Finally, we discuss the adversary who can control ESs (\mathcal{A}_{ES}). Note that \mathcal{A}_{ES} have the same capability as all prior adversary but the following theorem indicates that its view can still be simulated by ORAM parameters (N, Z, B, R):

THEOREM 3. *Let Π be the scheme of (**Setup**, **Upload**, **Fetch**, **Sync**). The adversary on ES (\mathcal{A}_{ES}) chooses the Path ORAM and rORAM parameters (N, Z, B, R) for **Setup** and selects a list of same-length videos for the CDN service provider to **Upload**. Later, \mathcal{A}_{ES} can arbitrarily **Fetch** videos and observe the blocks sent in and out on ES . OblivCDN ensures that ES is data-oblivious against the adversary, assuming that rORAM is data-oblivious, the PRF constructions is secure, and the permutations are selected uniformly at random.*

We provide the proof for above theorems in Appendix C.4.

C.4 Security Analysis for OblivCDN Entities

We provide the security proof for each individual parts of OblivCDN, starting from *Enclave* in the *CP* (ref. Theorem 1) as follows:

PROOF. (*Security of the Enclave*). We follow the real/ideal paradigm to consider follow two games: In the real world game, \mathcal{A}_{CP} interacts with a real system implemented in the *CP*, called Π_{CP} , which runs the algorithms for *CP* as stated in Algorithm 1. In the ideal world game, \mathcal{A}_{CP} interacts with a simulator \mathcal{S}_{CP} simulating the system. In both experiments, the adversary provides the same ORAM parameters (N, Z, B, R) and can supply any number of same-length videos operated in **Upload**, **Fetch**, and **Sync** operations.

We start from the ideal world game, where the simulator can be constructed as follows:

Setup:

- (1) Runs the Path ORAM simulator \mathcal{S}_{ORAM} with N, Z, B to initiate data structures VideoMap and BlockStateMap;
- (2) Runs the rORAM simulator \mathcal{S}_{rORAM} with N, Z, B, R to initiate BlockTracker $_r$, $\forall r \in [0, \log_2 R]$;
- (3) Initiates flat arrays MetaStash $_r \forall r \in [0, \log_2 R]$;
- (4) Sends instructions to ESs to initialise the data structures with the same parameters;

Throughout the **Setup** process, \mathcal{A}_{CP} observer exactly the ORAM parameters N, Z, B, R from the memory allocations.

Upload:

- (1) Runs \mathcal{S}_{ORAM} to update VideoMap and BlockStateMap to track the states of newly added video and blocks;
- (2) Runs \mathcal{S}_{ORAM} to access BlockStateMap and get block states;
- (3) Selects randomly generated masks to encrypt all blocks;
- (4) Insert blocks into MetaStash $_r \forall r \in [0, \log_2 R]$ according to their state s ;
- (5) Write blocks into S_r on ES ;

The **Upload** process still reveals the ORAM parameters N, Z, B, R from the ORAM accesses as it always read fixed $\log_2 N \times Z$ blocks for metadata accesses. It additionally leaks range 2^r for each rORAM tree and stash since it always access 2^r blocks in those data structures. No information will be revealed from the video blocks sent out to ES since they are encrypted by random masks.

Fetch:

- (1) Runs \mathcal{S}_{ORAM} to load *bid* and states of given video ID from VideoMap and BlockStateMap;

- (2) Sends the information to *Subscribers*;
- (3) Runs \mathcal{S}_{rORAM} to simulate the process of fetching *bids* from BlockTracker $_r$ to MetaStash $_r$;
- (4) Runs \mathcal{S}_{ORAM} to access BlockStateMap and get block states for blocks added into BlockTracker $_r$;
- (5) Refers to the block state changes from \mathcal{S}_{rORAM} to runs DPF simulator \mathcal{S}_{DPF} to generate 2^r key pairs;
- (6) Selects 2^r random masks as the re-encryption keys;
- (7) Combines DPF key, random masks and block states as 2^r BlockRangeRet tokens and sends to CSs ;
- (8) Runs \mathcal{S}_{ORAM} to update the block states in BlockStateMap;
- (9) Generates $|S_r|$ random permutations to permute MetaStash $_r$;
- (10) Selects $|S_r|$ random masks as the re-encryption keys;
- (11) Combines permutations and random masks as $|S_r|$ PerReFunc tokens and sends to CSs ;
- (12) Runs \mathcal{S}_{ORAM} to update the block states in BlockStateMap;

During **Fetch**, the *Enclave* reveals the ORAM parameters N, Z, B, R from the ORAM accesses on its metadata as well as the number of tokens sent to CSs . Furthermore, it reveals range 2^r for each rORAM tree and stash from the above process. Nonetheless, the token itself does not reveal any extra information, because the DPF key is simulated via the input field size, which is $|S_r| + \log_2 N \times Z$ (depicted by ORAM parameters), the masks/permutations are selected randomly, and the location information (path, offset, and new ID) inside are simulated via the rORAM simulator \mathcal{S}_{rORAM} .

Sync:

- (1) Runs \mathcal{S}_{rORAM} to simulate the process of fetching all 2^r paths from BlockTracker $_r$ to MetaStash $_r$;
- (2) Runs \mathcal{S}_{ORAM} to access BlockStateMap and get block states for blocks added into BlockTracker $_r$;
- (3) Refers to the block state changes from \mathcal{S}_{rORAM} to select $2^r \times \log_2 N \times Z$ random permutations;
- (4) Selects $2^r \times \log_2 N \times Z$ random masks as the re-encryption keys;
- (5) Combines permutations and random masks as $2^r \times \log_2 N \times Z$ PathRangeRet tokens and sends to CSs ;
- (6) Runs \mathcal{S}_{ORAM} to update the block states in BlockStateMap;
- (7) Runs \mathcal{S}_{rORAM} to simulate the process of evicting *bids* from MetaStash $_r$ to 2^r paths in BlockTracker $_r$;
- (8) Refers to the block state changes from \mathcal{S}_{rORAM} to runs DPF simulator \mathcal{S}_{DPF} to generate $2^r \times \log_2 N \times Z$ key pairs;
- (9) Selects $2^r \times \log_2 N \times Z$ random masks as the re-encryption keys;
- (10) Combines DPF key, random masks and block states as $2^r \times \log_2 N \times Z$ PriRangeEvict tokens and sends to CSs ;
- (11) Runs \mathcal{S}_{ORAM} to update the block states in BlockStateMap;

The **Sync** process also reveals the ORAM parameters N, Z, B, R and range 2^r of rORAM tree and stash from the ORAM accesses on its metadata as well as the number of tokens sent to CSs . On the other hand, the tokens do not reveal extra information as they are all simulated with ORAM parameters or sampled uniformly at random.

We now prove that the view generated by \mathcal{S}_{CP} in the ideal world is indistinguishable from the real world execution of Π_{CP} , which runs the algorithms for *CP* as stated in Algorithm 1, against the adversary \mathcal{A}_{CP} . The following sequence of hybrid executions $\mathcal{H}_0, \dots, \mathcal{H}_3$ gradually change invocations of the simulators to real

sub-protocols, which demonstrates that the above ideal world execution is indistinguishable from the real-world as long as all sub-protocols are proven to be secure:

Hybrid 0. We start with the ideal world as our initial hybrid, \mathcal{H}_0 .

Hybrid 1. **Hybrid 1** is the same as **Hybrid 0**, except that the simulator \mathcal{S}_{CP} uses real PRP/PRF outputs to replace the permutations and encryption/re-encryption keys for **Upload**, **Fetch**, and **Sync**. Security of pseudorandom functions holds that \mathcal{A}_{CP} 's advantage in distinguishing \mathcal{H}_0 from \mathcal{H}_1 is $negl(\lambda)$.

Hybrid 2. **Hybrid 2** is the same as **Hybrid 1**, except that the simulator \mathcal{S}_{CP} uses a real DPF scheme to generate DPF keys in the tokens during **Fetch** and **Sync**. The DPF security ensures that \mathcal{A}_{CP} 's advantage in distinguishing \mathcal{H}_1 from \mathcal{H}_0 is $negl(\lambda)$.

Hybrid 3. **Hybrid 3** is the same as **Hybrid 2**, except that the simulator \mathcal{S}_{CP} uses a real Path ORAM/rORAM instance to enable access pattern hiding access. Accordingly, subsequent accesses on the same-length requests cause the same distribution of RAM access patterns. Security of Path ORAM and rORAM implies that \mathcal{A}_{CP} 's advantage in distinguishing \mathcal{H}_3 from \mathcal{H}_2 is $negl(\lambda)$.

The above hybrid executions show that the simulated view is indistinguishable from the real world. Hence, we can conclude that the *Enclave* in the *CP* is data-oblivious, and \mathcal{A}_{CP} cannot infer sensitive information via memory access side-channels. \square

For the adversary on *CSs*, we will have the following proof for Theorem 2:

PROOF. (*Security of the CS*). We follow the real/ideal paradigm to consider follow two games: In the real world game, an adversary \mathcal{A}_{CS_p} interacts with a real implementation of $CS_{p \in \{1,2\}}$, running the algorithms Π_{CS_p} as stated in Algorithm 1, which consist of PathRangeRet, PriRangeEvict, PerReFunc, and BlockRangeRet. In the ideal world game, \mathcal{A}_{CS_p} interacts with a simulator \mathcal{S}_{CS_p} simulating the system. In both experiments, the adversary provides the same ORAM parameters (N, Z, B, R) and can supply any number of same-length videos operated in **Upload**, **Fetch**, and **Sync** operations.

Again, we start from the ideal world game, where the simulator can be constructed as follows⁶:

At the beginning of the simulation, the adversary chooses the CS_p to compromise, denoted $ComID \in \{1, 2\}$. Then,

Fetch:

- (1) Receives 2^r simulated tokens from the *CP* for BlockRangeRet;
- (2) For each token, retrieves $\log_2 N$ blocks from the designated path of E_r , the simulator responds with $\log_2 N$ random blocks for each requests;
- (3) Runs BlockRangeRet against retrieved blocks;
- (4) Writes the result blocks to the designated locations of S_r . The simulator runs \mathcal{S}_{rORAM} to write the corresponding block according to the instructions.
- (5) Receives $|S_r|$ simulated tokens from the *CP* for PerReFunc;
- (6) If $ComID = 1$, retrieves the entire stash S_r and receives $|S_r|$ random blocks from the simulator, permutes/re-encrypt all blocks inside, and sends to CS_2 ;

⁶Note that \mathcal{S}_{CS_p} only receives information in **Fetch**, and **Sync** operations, so we omit **Setup** and **Upload** operations as \mathcal{A}_{CS_p} only submit its inputs (ORAM parameters and videos) but cannot obtain a view on those operations

- (7) If $ComID = 2$, retrieves $|S_r|$ blocks from CS_1 and receives $|S_r|$ random blocks from the simulator, permutes/re-encrypt all blocks inside, and store in S_r . The simulator applies the permutations and re-encryption keys to permute and re-encrypt the entire S_r locally;

During **Fetch**, \mathcal{A}_{CS_p} only can observe the number of tokens from the *CP* and number of blocks from the E_r and S_r , which directly correlates to the ORAM parameters. On the other hand, the tokens and blocks received does not reveal any information, as they are all simulated or randomly selected by the simulator via the ORAM parameters (see our proof for Theorem 5).

Sync:

- (1) Receives $2^r \times \log_2 N \times Z$ simulated tokens from the *CP* for PathRangeRet;
- (2) If $ComID = 1$, retrieves $2^r \times \log_2 N \times Z$ blocks from the designated locations of E_r , receives $2^r \times \log_2 N \times Z$ random blocks from the simulator, permutes/re-encrypt all blocks inside, and sends to CS_2 ;
- (3) If $ComID = 2$, retrieves $2^r \times \log_2 N \times Z$ blocks from CS_1 and receives $2^r \times \log_2 N \times Z$ random blocks from the simulator, permutes/re-encrypt all blocks inside, and store in S_r . The simulator runs \mathcal{S}_{rORAM} to retrieve the corresponding blocks from E_r to S_r according to the instructions;
- (4) Receives $2^r \times \log_2 N \times Z$ simulated tokens from the *CP* for PriRangeEvict;
- (5) Retrieves $2^r \times \log_2 N \times Z$ blocks from the designated locations of S_r , the simulator responds with $2^r \times \log_2 N \times Z$ random blocks for each requests;
- (6) Runs PriRangeEvict against retrieved blocks;
- (7) Writes the result blocks to the designated locations of E_r . The simulator runs \mathcal{S}_{rORAM} to write the corresponding block according to the instructions.

Similar to **Fetch**, \mathcal{A}_{CS_p} only can observe the number of tokens from the *CP* and number of blocks from the E_r and S_r , which directly correlates to the ORAM parameters in **Sync**. No information is revealed from the simulated tokens or randomly selected blocks.

We now ready to prove that the view generated by \mathcal{S}_{CS_p} in the ideal world is indistinguishable from the real world execution of Π_{CS_p} , which runs the algorithms for CS_p as stated in Algorithm 1, against the adversary \mathcal{A}_{CS_p} via the following sequence of hybrid executions $\mathcal{H}_0, \dots, \mathcal{H}_4$.

Hybrid 0. We start with the ideal world as our initial hybrid, \mathcal{H}_0 .

Hybrid 1. **Hybrid 1** is the same as **Hybrid 0**, except that the simulator \mathcal{S}_{CS_p} uses real PRP/PRF outputs to replace the permutations and encryption/re-encryption keys in the token. Security of pseudorandom functions holds that \mathcal{S}_{CS_p} 's advantage in distinguishing \mathcal{H}_0 from \mathcal{H}_1 is $negl(\lambda)$.

Hybrid 2. **Hybrid 2** is the same as **Hybrid 1**, except that the simulator \mathcal{S}_{CS_p} uses a real DPF scheme to generate DPF keys in the tokens. The DPF security ensures that \mathcal{S}_{CS_p} 's advantage in distinguishing \mathcal{H}_1 from \mathcal{H}_0 is $negl(\lambda)$.

Hybrid 3. **Hybrid 3** is the same as **Hybrid 2**, except that the simulator \mathcal{S}_{CS_p} forwards real blocks to CS_{ComID} upon the requests. Since all blocks are encrypted with one-time PRF masks, the security of PRF ensures that \mathcal{A}_{CS_p} 's advantage in distinguishing \mathcal{H}_3 from \mathcal{H}_2 is $negl(\lambda)$.

Hybrid 4. Hybrid 4 is the same as Hybrid 3, except that the simulator \mathcal{S}_{CS_p} uses real oblivious block routing protocols to replace \mathcal{S}_{rORAM} . For the compromised party CS_{ComID} , our prior discussion pinpoints that it only receives instructions generated from rORAM operations and observes random blocks locally. Meanwhile, it does not know actual block operations on ESs. Hence, \mathcal{A}_{CS_p} 's advantage in distinguishing \mathcal{H}_4 from \mathcal{H}_3 is $negl(\lambda)$.

The above hybrid executions show that the simulated view is computationally indistinguishable from the real world. Hence, we can conclude that the \mathcal{A}_{CS_p} cannot infer sensitive information via the view of compromised server. \square

Finally, we discuss the security of ESs against the adversary on \mathcal{A}_{ES} , in following proof for Theorem 3:

PROOF. (*Security of the ESs*). Similarly, we start from constructing a simulator to simulate the view of ES. Note that ES serves as data store and purely sends and receives blocks from other entities, which can be simply described as follows:

Setup:

- (1) Initialises $\log_2 R$ ORAM tree with $N \times Z \times B$ space;
- (2) Initialises $\log_2 R$ stash with $|S_r|$ space;

Upload:

- (1) Receives random blocks and put into S_r ;

Fetch:

- (1) Send requested 2^f blocks to *Subscribers* for each request
- (2) Send requested $2^f \times \log_2 N$ blocks from E_r to CS_1 ;
- (3) Receives 2^f random blocks and put into S_r ;
- (4) Sends $|S_r|$ blocks from S_r to CS_1 ;
- (5) Receives $|S_r|$ random blocks from CS_2 and put into S_r ;

Sync:

- (1) Send requested $2^f \times \log_2 N \times Z$ blocks from E_r to CS_1 ;
- (2) Receives $2^f \times \log_2 N \times Z$ random blocks and put into S_r ;
- (3) Sends $|S_r|$ blocks in S_r to CS_1 ;
- (4) Receives $2^f \times \log_2 N \times Z$ random blocks from CS_2 and put into E_r ;

From the above description, we can see that ES exactly implements what rORAM server did as in the original protocol [21]. In addition, data-oblivious on client-side structure S_r is ensured by random permutations. Hence, we can conclude that ES inherits the security guarantees of rORAM and is data-oblivious against the adversary who compromises ESs only. \square

C.5 Security Analysis for OblivCDN System

In this section, we take real-world deployment considerations into the security model and further discuss the following two cases: The first case is called colluding ESs, where the *CDN service provider* deploys one CS on the *ISP partner* who hosts ESs, which will further enable the *ISP partner* to collect information from CS. Nonetheless, the following theorem indicates that the above adversary (denoted as \mathcal{A}_{ISP}) cannot learn extra information other than the ORAM parameters (N, Z, B, R) as far as it only can compromise one CS.

THEOREM 4. *Let Π be the scheme of (Setup, Upload, Fetch, Sync). The adversary on the ISP partner (\mathcal{A}_{ISP}) chooses the Path ORAM and rORAM parameters (N, Z, B, R) for Setup and selects a list of*

same-length videos for the CDN service provider to Upload. Later, \mathcal{A}_{ISP} can arbitrarily Fetch videos and observe the tokens/blocks sent in and out on one CS and ES. OblivCDN is data-oblivious against the \mathcal{A}_{ISP} , assuming that rORAM is data-oblivious, the DPF and PRF constructions are secure, and the permutations are selected uniformly at random.

PROOF. In this proof, we firstly describe how to construct a simulator to simulate the view of \mathcal{A}_{ISP} .

At the beginning of the simulation, the adversary still chooses the CS_p to compromise, denoted $ComID \in \{1, 2\}$. Then,

Setup:

- (1) Initialises $\log_2 R$ ORAM tree with $N \times Z \times B$ space;
- (2) Initialises $\log_2 R$ stash with $|S_r|$ space;

Upload:

- (1) Receives random blocks and put into S_r ;

Fetch:

- (1) Receives 2^f simulated tokens from the CP for BlockRangeRet;
- (2) For each token, retrieves $\log_2 N$ blocks from the designated path of E_r
- (3) Runs BlockRangeRet against retrieved blocks;
- (4) Writes the result blocks to the designated locations of S_r .
- (5) Receives $|S_r|$ simulated tokens from the CP for PerReFunc;
- (6) If $ComID = 1$, retrieves the entire stash S_r , permutes/re-encrypt all blocks inside, and sends to CS_2 ;
- (7) If $ComID = 2$, retrieves $|S_r|$ blocks from CS_1 and receives $|S_r|$ random blocks from the simulator, permutes/re-encrypt all blocks inside, and store in S_r . The simulator applies the permutations and re-encryption keys to permute and re-encrypt the entire S_r locally;

Sync:

- (1) Receives $2^f \times \log_2 N \times Z$ simulated tokens from the CP for PathRangeRet;
- (2) If $ComID = 1$, retrieves $2^f \times \log_2 N \times Z$ blocks from the designated locations of E_r , permutes/re-encrypt all blocks inside, and sends to CS_2 ;
- (3) If $ComID = 2$, retrieves $2^f \times \log_2 N \times Z$ blocks from CS_1 and receives $2^f \times \log_2 N \times Z$ random blocks from the simulator, permutes/re-encrypt all blocks inside, and store in S_r . The simulator runs \mathcal{S}_{rORAM} to retrieve the corresponding blocks from E_r to S_r according to the instructions;
- (4) Receives $2^f \times \log_2 N \times Z$ simulated tokens from the CP for PriRangeEvict;
- (5) Retrieves $2^f \times \log_2 N \times Z$ blocks from the designated locations of S_r ;
- (6) Runs PriRangeEvict against retrieved blocks;
- (7) Writes the result blocks to the designated locations of E_r .

For the above description, we can see that the simulation is exactly the same as the simulator of CS_p when replacing the \mathcal{S}_{rORAM} with real oblivious block routing operations. This is because we have proven that the view on ESs is indistinguishable from the view of the rORAM server in Theorem 3. It means that for an adversary who compromises CS_p , it cannot learn extra information by additionally compromising ESs, and vice versa. Hence, the adversary \mathcal{A}_{ISP} does not gain extra advantage than \mathcal{A}_{CS_p} , and OblivCDN is still data-oblivious against the new adversary. \square

Table 10: Computation costs (second) $|B| = 2$ KB

Building Block	CP	CS ₁	CS ₂	$E_{r=8}$ & $S_{r=8}$
BlockRangeRet	0.1	0.031	0.028	1.5
PerReFunc	8.5	2.2	2.7	0.2
PathRangeRet	6.7	1.07	1.3	1.7
PriRangeEvict	5.3	368.5	369.5	0.2

Table 11: Computation costs (second) $|B| = 4$ KB

Building Block	CP	CS ₁	CS ₂	$E_{r=8}$ & $S_{r=8}$
BlockRangeRet	0.1	0.057	0.063	2.6
PerReFunc	8.5	4.5	5.4	0.25
PathRangeRet	6.7	2.1	2.6	2.9
PriRangeEvict	5.3	735.3	737.3	0.23

We further discuss the case where the *CDN service provider* employs *CP* and one *CS_p* on the two servers from the same *cloud service provider*. In this case, the adversary (\mathcal{A}_{CSP}) can further observe the memory access pattern and tokens from *CP*, as well as the oblivious block routing process on *CS_p*. The following theorem captures the security of OblivCDN against \mathcal{A}_{CSP} :

THEOREM 5. *Let Π be the scheme of (Setup, Upload, Fetch, Sync). The adversary on the cloud service provider (\mathcal{A}_{CSP}) chooses the Path ORAM and rORAM parameters (N, Z, B, R) for Setup and selects a list of same-length videos for the CDN service provider to Upload. Later, \mathcal{A}_{CSP} can arbitrarily Fetch videos and observe the access pattern on CP and the tokens/blocks sent in and out on one CS. OblivCDN is data-oblivious against the \mathcal{A}_{CSP} , assuming that rORAM is data-oblivious, the DPF and PRF constructions are secure, and the permutations are selected uniformly at random.*

PROOF. Since the proof structure for Theorem 5 is similar to that for Theorem 4, we provide a proof sketch here. In particular, the simulator for \mathcal{A}_{CSP} aims to generate a joint view on the access pattern of *CP* for all OblivCDN operations and the tokens/blocks sent to/by *CS_p* under the given instructions. Since the access pattern on *CP* is oblivious, the above view is exactly the same as the simulator of *CS_p* when replacing the simulated tokens with real tokens generated by PRF/PRP/DPF instances (i.e., **Hybrid 3** for Theorem 2). This means that for an adversary who compromises *CS_p*, it cannot learn extra information by additionally compromising *CP*, and vice versa. As a result, the adversary \mathcal{A}_{CSP} does not gain extra advantage than \mathcal{A}_{CS_p} , and OblivCDN is still data-oblivious against the new adversary. \square

D COST BREAKDOWN FOR BUILDING BLOCKS

We show the breakdown operation costs of the *CP* (with the *Enclave* included), each of $CS_{p \in \{1,2\}}$, and the *ES* involved in the four oblivious building blocks. Table 10 and 11 show the costs when executing the building blocks in the ORAM E_r and its stash S_r with $r = 8$, which support the range access of 2^8 blocks with block size 2 and 4 KB, respectively.

The highest computation cost of CS_1 and CS_2 in the PriRangeEvict is due to the DPF evaluation to write $2^r \times \log_2 N \times Z$ blocks to 2^r ORAM paths, and each block write requires to scan $|S_r| = 105 \times 2^r$ blocks. Other building blocks only work on fewer blocks

(i.e., $2^r \times \log_2 N$ blocks for BlockRangeRet, and $|S_r|$ blocks for PerReFunc) or has less operations on blocks, i.e., BlockRangeRet can permute and re-encrypt a path of $\log_2 N \times Z$ blocks with one scan.

The communication cost breakdowns under different rORAM parameters (r) are given in Figure 14.

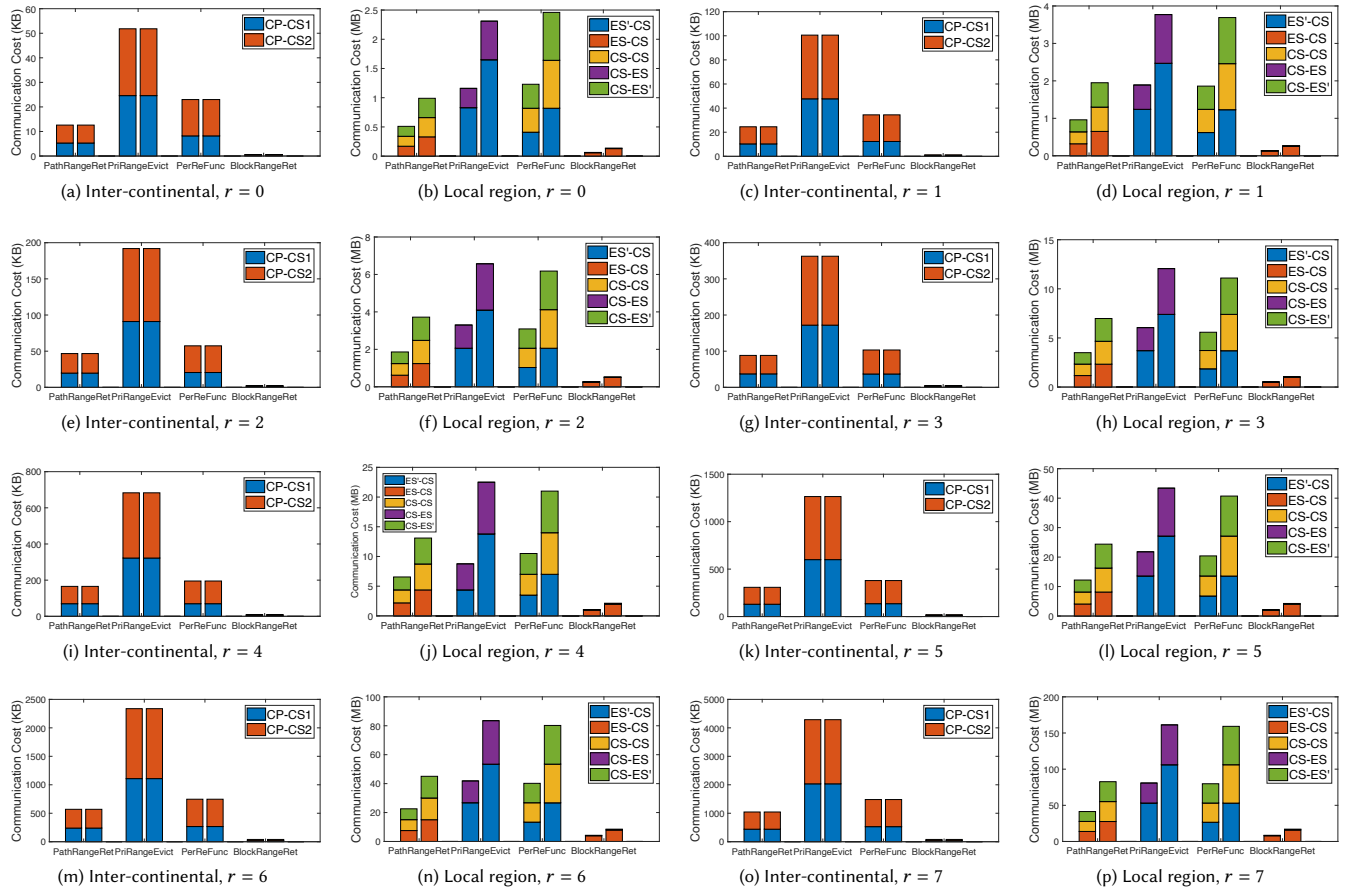


Figure 14: The communication cost (MB) of oblivious operations with varying r . For each operation, the left bar is for $|B| = 2$ KB, and the right one is for $|B| = 4$ KB.